

Review

Not peer-reviewed version

---

# Optical Immunosensors for Bacteria Detection in Food Matrices

---

Dimitra Kourti , [Michailia Angelopoulou](#) <sup>\*</sup> , [Panagiota Petrou](#) , [Sotirios Kakabakos](#)

Posted Date: 29 June 2023

doi: 10.20944/preprints202306.2108.v1

Keywords: immunosensor; optical detection; bacteria



Preprints.org is a free multidiscipline platform providing preprint service that is dedicated to making early versions of research outputs permanently available and citable. Preprints posted at Preprints.org appear in Web of Science, Crossref, Google Scholar, Scilit, Europe PMC.

Copyright: This is an open access article distributed under the Creative Commons Attribution License which permits unrestricted use, distribution, and reproduction in any medium, provided the original work is properly cited.

Review

# Optical Immunosensors for Bacteria Detection in Food Matrices

Dimitra Kourti, Michailia Angelopoulou \*, Panagiota Petrou and Sotirios Kakabakos

Immunoassays/Immunosensors Lab, Institute of Nuclear & Radiological Sciences & Technology, Energy & Safety, NCSR "Demokritos" Aghia Paraskevi 15341, Greece; dimkourti96@gmail.com (D.K); ypetrou@rrp.demokritos.gr (P.P.); skakab@rrp.demokritos.gr (S.K.)

\* Correspondence: mikangel@ipta.demokritos.gr; Tel.: +302106503861

**Abstract:** Optical immunosensors are one of the most popular category of immunosensors with applications in many fields including diagnostics, environmental and food analysis. The latter field is of particular interest not only for the scientists but also for the regulatory authorities and the public since food is essential for life but can be also the source of many health problems. In this context, the current review aims to provide an overview of the different types of optical immunosensors focusing onto their application for the determination of pathogenic bacteria in food samples. In particular, after the description of main optical transduction techniques, their implementation for the immunochemical determination of bacteria will be discussed. Finally, a short commentary about the future trends in optical immunosensors for food safety applications will be provided.

**Keywords:** immunosensor; optical detection; bacteria

## 1. Introduction

Foodborne diseases affect according to World Health Organization (WHO) 1 in 10 people every year worldwide [1], with symptoms ranging from mild diarrhea to severe complications and even death [2]. According to WHO, it was estimated that the cases of food poisoning reached up to 600 million, with 420.000 deaths worldwide, amongst which 125.000 are children under the age of 5 [1]. Especially, pathogenic bacteria play a crucial role in food poisoning with the majority of the incidents to be caused by 15 pathogenic bacteria including *Listeria monocytogenes*, *Escherichia coli* O157:H7, *Clostridium botulinum*, *Legionella pneumophila*, *Campylobacter jejuni*, *Salmonella* spp., *Staphylococcus aureus*, *Shigella*, *Vibrio vulnificus* and *Bacillus cereus* [3]. Most of these bacteria are detected in dairy products, fresh vegetables, raw products and undercooked meat and seafood [4, 5].

The efficiency and reliability of the techniques employed to detect these pathogens in food matrices are of paramount importance for the prevention of foodborne diseases. [6, 7]. The conventional methods for bacteria detection and identification are based on culturing and colony counting. Those methods are reliable, sensitive, and are considered as the "gold standard" for detecting the presence of bacteria, however, they require prior to detection several steps such as pre-enrichment, selective enrichment, isolation and confirmation through biochemical and serological tests [8, 9]. Thus, there was an urgent need for rapid bacteria detection techniques, that led to the development of new methods such as molecular and immunological ones [10]. Molecular methods rely on polymerase chain reaction (PCR) [11–13] to rapidly and effectively identify various bacteria through their genetic fingerprinting. On the other hand, immunoassays rely on antibodies that recognize specific proteins or liposaccharides of bacteria external membrane. Chemiluminescent Enzyme Immunoassay (CL-EIA) [14] and Enzyme-Linked-Immunosorbent Assay (ELISA)[15–17] are the immunochemical methods most widely employed for rapid bacterial detection and quantification. Immunoassays are characterized by high sensitivity and accuracy, simple sample preparation and low cost of instrumentation compared to other instrumental methods such as chromatographic ones. Nonetheless, these methods are laboratory bound since they involve multiple processing steps and desktop instrumentation [18, 19]. The quest for portable analytical devices that could provide reliable results in short analysis time and be suitable for on-site applications has been

the driving force behind the development of biosensors. Nowadays, the realization of biosensor systems that combine outstanding analytical performance with portability has moved from the sphere of fiction to reality due to the significant progress in the field of nanotechnology that enabled the fabrication of such sensors [20]. Thus, modern biosensor technologies can provide high detection sensitivity and specificity, high-speed analysis, and quantitative results in real-time [21]. Biosensors are defined by IUPAC as analytical devices that provide quantitative or semi-quantitative information by combining a biological recognition element with a physicochemical transducer, that transforms the biorecognition event into a physically detectable signal [22]. The recognition element can be any bioreceptor [23], such as nucleic acid probe, aptamer, phage, antibody, antigen, whole cell, enzyme, etc., that can bind the target molecule specifically and with high affinity [24–31] (Figure 1a).

Immunosensors, i.e., biosensors that rely on antibody-antigen reactions for analyte detection, are the most abundant category of biosensors due to the indispensable ability of antibodies for highly selective detection of the targeted analytes in complex media and the versatility of available assay formats that could be successfully employed for the determination of both low- and high-molecular weight analytes, such as bacteria [31]. They can be divided according to the transduction principle to electrochemical [32–35], piezoelectric [36–38] or optical ones [32, 39], which can detect biological interactions by evaluating the variations in the electrical signal, mass or light, respectively (Figure 1b). Electrochemical immunosensors are cost-efficient devices and have the potential for miniaturization. Nevertheless, they lack in sensitivity and often require labels for signal enhancement to improve their detection limits. Similarly, immunosensors based on piezoelectric phenomena, even though are suitable for label-free detection, they are characterized in general by relatively low detection sensitivity [40]. On the other hand, optical immunosensors exhibit high sensitivity and offer for simple, fast and accurate detection of a great variety of analytes, including bacteria [41]. Optical detection methods (Figure 1b) are based on different transduction principles such as light absorbance, total internal reflectance, photoluminescence, fluorescence, light polarization, interferometry, Raman scattering and surface plasmon resonance [42,43].

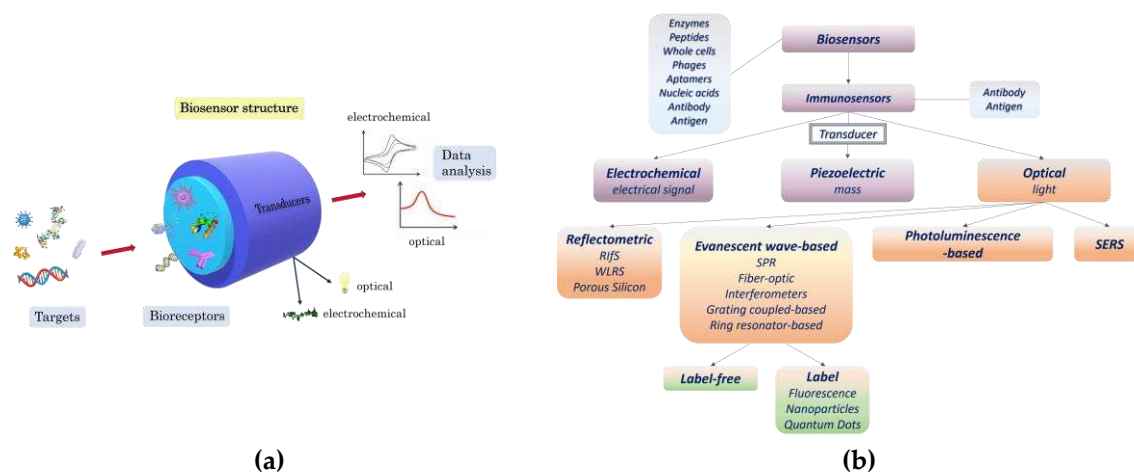


**Figure 1.** (a) Schematic of a biosensor. (b) The different categories of biosensors.

The scope of this review is to summarize the achievements of optical immunosensors for foodborne bacteria detection. At first, short descriptions of the different detection principles employed will be provided. Then, the application of optical immunosensors for bacteria detection in different food matrices will be extensively presented. Finally, a short commentary on the future trends regarding the prospective applications and challenges of optical immunosensors in food analysis is included.

## 2. Principles of optical immunosensors

### 2.1. Assay formats

In principle, most immunosensors could offer the potential to monitor directly the antigen-antibody binding in real-time. Such direct detection although is simpler and faster, since there is no need for additional reaction steps, is usually limited to high-molecular weight analytes, for which the antigen-antibody reaction results in a measurable change of sensor response [32]. Therefore, in most immunosensors the assay formats usually applied in microtiter plate solid-phase immunoassays are followed, i.e., the competitive or the non-competitive assay format. For the low-molecular weight analytes including toxins, pesticides, antibiotics, pharmaceutical residues, etc., the preferred assay format is the competitive one, based either on immobilized antibody (Figure 2a) or on immobilized antigen or analyte-protein conjugate (Figure 2b). In the first approach, the antibody is immobilized onto the transducer surface and the concentration of the analyte is defined through its competition with a labelled analyte' or analyte-protein conjugate for binding to the antibody. In the second approach, the analyte is immobilized onto the transducer surface (either directly or as an analyte protein conjugate) and competes with the analyte in the sample for the binding sites of the antibody. Although both approaches are applicable for a given analyte-antibody pair, the second might be advantageous regarding the stability of immobilized biomolecule, i.e., the analyte or analyte-protein conjugate, since antibodies are known to lose a great part of their functionality upon immobilization. The non-competitive or sandwich immunoassay format is suitable for high-molecular weight analytes, which have at least two antigenic determinants or epitopes in their molecule. This means, that at least two antibodies recognizing two different parts of the analyte are available. This is essential for the realization of a non-competitive assay, since as depicted in Figure 2c, an antibody immobilized onto the transducer surface (usually referred as capture antibody) binds the antigen-analyte through one epitope and a second antibody (referred as detection or reporter antibody) is attached on a different epitope forming a "sandwich" with the antigen. The detection antibody can be labelled or not depending on the transduction principle involved.

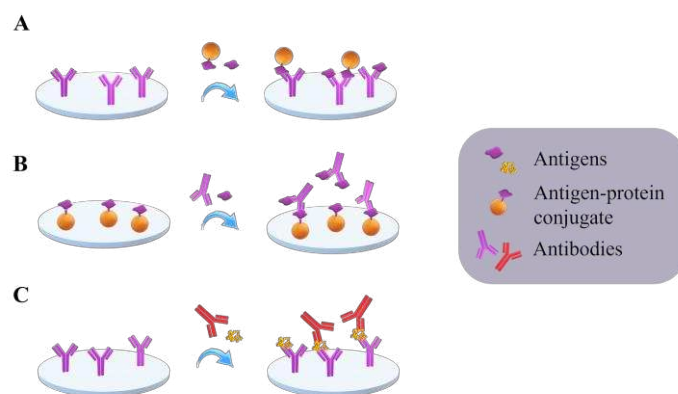


**Figure 2.** Schematic presentation of different immunoassay formats applied to optical immunosensors.

### 2.2. Main optical transduction principles

The optical transduction principles can be divided into two main categories, those involving labels and the label-free ones.

#### 2.2.1. Detection using labels

A significant number of optical immunosensors are based on use of labels such as fluorescent organic dyes, gold nanoparticles or quantum dots for the quantification of antibody-analyte reaction

and the determination of analyte concentration in a sample [44]. Biosensing using fluorescently labelled molecules and optical fibers was amongst the first optical transduction principles to be explored [45]. Apart from the typical cylindrical optical fibers, planar waveguides and capillaries that enabled light propagation through total internal reflection have been also employed as transducers for the development of optical fluorescence immunosensors [46, 47]. Over the years, metal nanoparticles have been employed as labels and incorporated in immunochromatographic strips or used as liquid phase reagents to obtain semi-quantitative, relying on visual evaluation, or quantitative results through implementation of an instrument that could quantitate the color, fluorescence or chemiluminescence intensity. The latter can be performed using smartphones as detection, signal processing, and transmission apparatus moving the realization of portable devices a step forward [48].

### 2.2.2. Label-free detection

Label-free optical biosensing on the other hand, is based almost exclusively on monitoring the refractive index changes of the layer in close contact with the optical transducer due to immunochemical reactions [37]. There are two main categories of label-free optical transduction principles, the refractometric and the reflectometric ones [49]. In refractometric immunosensors, the light that is transmitted through a waveguide creates an electromagnetic field, known as evanescent field (Figure 3), that extends in the medium above the biosensor surface. This field is influenced by refractive index changes over the transducer surface due to biomolecular layer thickness increase caused by the immunoreaction. Thus, when the evanescent wave field is coupled back to the transducer, a change in the intensity, polarization or phase of the waveguided light is observed that is proportional to the concentration of analyte in the sample enabling its quantitative determination [50-52]. Transducers based on surface plasmon resonance (SPR), fiber optics, grating couplers, interferometers, and ring resonators fall in this category of optical sensors (Figure 4).

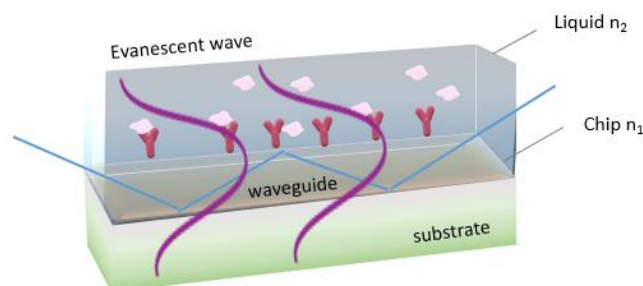


**Figure 3.** Schematic of the evanescent field sensing principle.

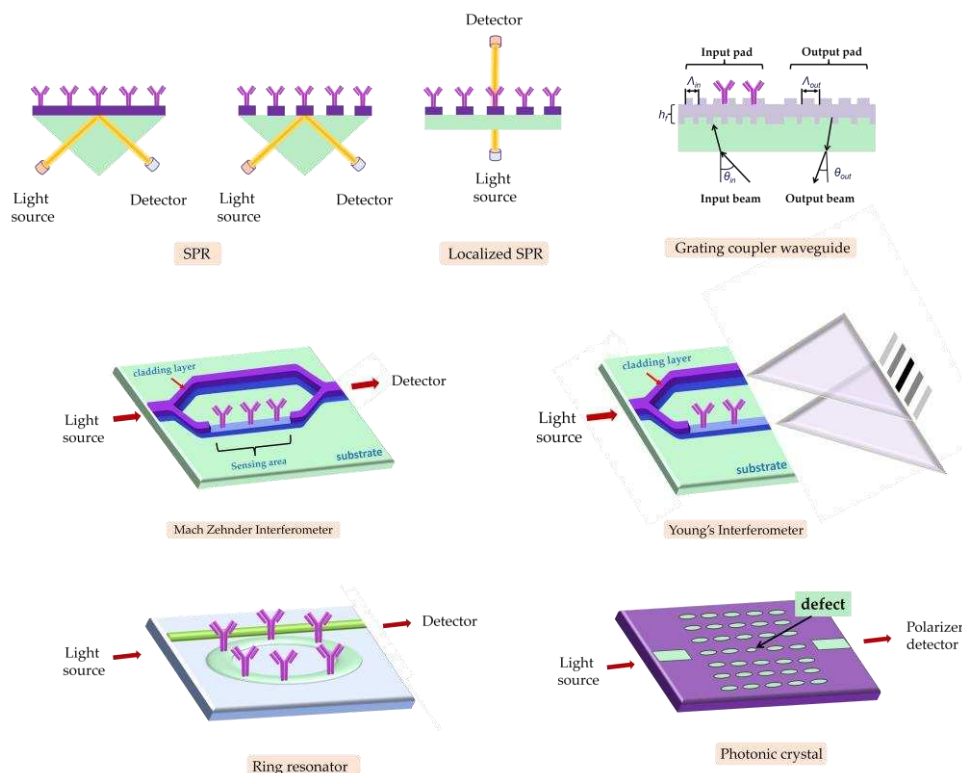


**Figure 4.** Schematic presentation of basic conformations of refractometric label-free optical transducers including SPR and localized SPR, grating coupler waveguides, interferometers, ring resonators, and photonic crystals.

Reflectometric sensors are based on light reflection by a stack of materials with different refractive indices leading to creation of an interference spectrum. The most widely explored reflectometric sensing method is the one introduced at 1991 by Gauglitz et al. [53], which is known as reflectometric interference spectroscopy (RIfS). RIfS transducers are made of a glass substrate on top of which a thin layer of transparent dielectric material has been deposited. Immunochemical reactions that take place on top of the dielectric layer are evidenced as shifts in the reflected interference spectrum. This spectrum is created due to reflection of the light beam at each interface of different refractive index with a slightly different angle leading to either constructive or destructive interference. The spectrum shift is directly correlated to the increase of biomolecular layer thickness due to immunoreaction and therefore it can be correlated to the analyte concentration in the sample through a calibration curve. Since the first report of RIfS sensors, a lot of progress has been made to the direction of reducing the cost and size of the instrumentation and increase the multiplexing capabilities, e.g., by monitoring, instead of the whole spectrum, specific wavelengths [54] or even a single wavelength [55]. In addition, other material combinations have been employed as transducers including porous silicon with or without thermally grown oxide [56], porous silicon-carbon composites [57], other porous materials such as  $\text{TiO}_2$  [58], or non-transparent substrates such as silicon with a transparent dielectric composed of silicon dioxide [59-61] or silicon nitride [62].

### 3. Application of optical sensors for bacteria detection

#### 3.1. Evanescent wave-based biosensors

##### 3.1.1. SPR immunosensors

Surface plasmon resonance (SPR) based immunosensors are the optical biosensors most frequently used for single or multiplex, label-free foodborne pathogenic bacterial detection due to

their high detection sensitivity and monitoring of binding reactions in real-time. The SPR phenomenon relies on excitation of metal free electrons (surface plasmons) when polarized light strikes at a certain angle a metal layer (usually gold) deposited on the surface of an optically transparent material (prism, grating coupler or dielectric waveguide). The excited plasmons create an evanescent wave field at the solution/gold interface. This wave is very sensitive to refractive index changes at the gold layer surface occurring due to a biomolecular reaction, and as a result, the angle of incident light has to change during the course of the reaction to preserve the surface plasmon wave, providing the means to monitor in real-time these reactions. Thus, it is possible to monitor both the immobilization of specific biomolecules (e.g., antibodies) as well as the binding of analyte to them in real-time (Figure 5) [41, 44].

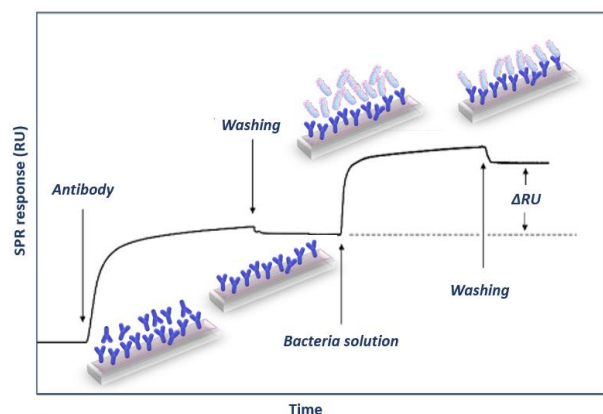


**Figure 5.** SPR response during the binding of a bacteria-specific antibody onto the biosensor surface followed by capturing of bacteria to the immobilized antibody.

The first report regarding detection of bacteria with an SPR sensor is dated back to 1998 [63], and was based on a sandwich immunoassay for detection of *Escherichia coli* O157:H7. The sensor was modified with protein A or protein G and a mouse monoclonal or a rabbit polyclonal antibody, respectively, was then immobilized. Depending on the antibody used for detection, LODs in the range  $5\text{--}7 \times 10^7$  cfu/mL have been achieved. *Vibrio cholerae* O1 was also identified with an SPR biosensor functionalized with a protein G layer [64]. The sensor chip was modified with a self-assembled monolayer of a mixture of 11-mercaptopundecanoic acid and hexanethiol on which protein G was covalently bound and used to immobilize a monoclonal antibody specific to *V. cholera* O1. The LOD of the assay was  $10^5$  cfu/mL. The same antibody immobilization approach was employed to immobilize onto SPR chips an antibody against *Legionella pneumophila* achieving a LOD of  $10^5$  cfu/mL [65]. *Salmonella enterica* serovar Enteritidis and *Escherichia coli* have been detected in spiked skim milk by a direct binding assay on SPR chips modified with protein G to which the anti-bacteria specific antibodies were then bound [66]. The LOD achieved after 1-h assay was 25 cfu/mL for *E. coli* and 23 cfu/mL for *Salmonella*. Detection of *Salmonella* groups B, D and E with SPR has been also reported employing a sandwich assay format and using antibody pairs from different animals [67]. It was found that the LOD improved 200 times compared to direct detection [67]. The benefits of the sandwich immunoassay format for bacteria detection have been also demonstrated in a study for detection of *Staphylococcus aureus* with SPR, where the LOD was improved from  $1 \times 10^7$  to  $1 \times 10^5$  cfu/mL when a sandwich immunoassay format was followed instead of direct detection [68]. In another report, where the direct binding assay was compared to a sandwich assay for detection of *E. coli* O157:H7, a 1000-fold improvement in sensitivity was reported leading to an LOD of  $10^3$  cfu/mL [69]. The immobilization of the polyclonal antibody against *E. coli* was performed through covalent bonding to a monolayer of mixed thiol-terminated polyethylene glycol with alkane or carboxyl-group ends. In another report, the free amine groups of protein A were converted to thiol groups, through reaction with 2-iminothiolane, to facilitate its immobilization onto SPR chips, which are then

modified with an antibody against *Salmonella paratyphi* [70]. A LOD of  $10^2$  cfu/mL was achieved employing the antibody modified chip in a direct binding assay. In another study, the SPR chip was modified with brushes of poly(carboxybetaine acrylamide) to reduce the non-specific binding of bacteria to its surface, while antibody modified gold nanoparticles were used as labels to increase the detection sensitivity [71]. This immunosensor could detect *E. coli O157:H7* in hamburger and cucumber samples at concentrations as low as 57 and 17 cfu/mL and *Salmonella* spp. at  $7.4 \times 10^3$  and  $11.7 \times 10^3$  cfu/mL, respectively [71]. Gold nanoparticles modified with an antibody against *Campylobacter jejuni* were also employed as labels in an SPR sandwich immunoassay that allowed the detection of this bacterium at concentrations as low as  $4 \times 10^4$  cfu/mL [72]. A gold-labelled secondary antibody was also employed to increase the detection sensitivity in a sandwich SPR for *L. monocytogenes* by 2-4 orders of magnitude compared to the direct binding assay, providing a LOD of  $10^2$  cfu/mL [73]. In another study, in order to achieve signal enhancement, a precipitate 3,3',5,5'-tetramethylbenzidine (TMB) substrate was used in combination with an antibody labelled with horse radish peroxidase (HRP) to detect bacteria captured by an antibody attached to SPR chip through covalent bonding to a self-assembled monolayer of mercaptoundecanoic acid [74]. Following this approach, a 250% signal enhancement was achieved with respect to the assay not employing the HRP/TMB system leading to a LOD of  $10^4$  cfu/mL for detection of *E. coli* in spinach leaves [74]. SPR chips have been modified in a plasma reactor in presence of cyclopropylamine vapors to induce reactive moieties containing nitrogen which were in turn used to immobilize antibodies using glutaraldehyde activation [75]. The chips were employed to detect *Salmonella typhimurium* by a direct binding assay that provided a LOD of  $10^5$  cfu/mL.

Along with the optimization of the SPR assays for bacteria detection, effort was devoted to sample treatment methods aiming either to improve detection sensitivity or alleviate non-specific matrix effects. For example, the performance of an SPR sensor for the detection of live, heat-killed, or detergent-lysed *E. coli O157:H7* cells was investigated and LODs of  $10^6$ ,  $10^5$ , and  $10^4$  cfu/mL, respectively, were reported [76]. The differences observed were ascribed to changes in cell size and morphology upon treatment with ethanol, whereas treatment with detergent led probably to fragmentation of cells to smaller particles that were recognized more efficiently by the antibody. The effect of sample preparation method was also evident in another study for detection of *E. coli O157:H7* in different food samples [77]. In this study, milk, apple juice, and ground beef patties were spiked with *E. coli O157:H7* at various concentrations and then analyzed with a portable SPR instrument commercialized by Texas Instruments Inc. under the tradename SPREETA™. The sensor chip was modified with neutravidin to enable immobilization of biotinylated antibodies against *E. coli O157:H7*. The spiked milk and apple juice samples were run without pretreatment, whereas the ground beef sample was extracted with buffer and homogenized prior to analysis. The LODs achieved ranged from  $10^2$ – $10^3$  cfu/mL depending on the sample analyzed. In another report, where a sandwich SPR assay for *Salmonella* with LOD of  $1.25 \times 10^5$  cells/mL was developed [78], the authors claimed that the presence of milk did not affect the assay performance alleviating the need for sample preparation or clean-up steps.

It has been suggested that the detection of whole bacteria using SPR generally results in lower sensitivity compared to other techniques, due to the limited penetration of bacteria by the electromagnetic field and the small difference of refractive index between bacterial cytoplasm and the surrounding aqueous medium [79]. Thus, instead of running over the sensor the sample, the sample is incubated with the pathogen specific antibody and after separation of free from bound antibody, the free antibody is quantified. This assay format is known as subtraction inhibition assay (SIA) and has been applied for the detection of *L. monocytogenes* [80], *E. coli O157:H7* [81], and *B. anthracis* spores [82]. The LODs reported were  $1 \times 10^5$ ,  $3.0 \times 10^4$ , and  $10^4$  cfu/mL, respectively, and were one order of magnitude lower than those achieved with the direct binding assay. The SIA format was also applied for the detection of fungal cells that are considerably larger than the bacterial ones [83]. Thus, it has been applied for the detection of sporangia of *Phytophthora infestans* [83], and of *Puccinia striiformis* with LODs of  $2.2 \times 10^6$  sporangia/mL and  $3.1 \times 10^5$  urediniospores/mL, respectively [84]. A

similar assay format was also applied for the SPR detection of *Cryptosporidium parvum* oocysts with a LOD of  $1 \times 10^2$  oocysts/mL [85]. In a different approach for indirect bacteria detection by SPR, a polyclonal antibody against a cell extract enriched for the invasion-associated protein, internalin B, was used to develop an inhibition assay for *Listeria monocytogenes* [86]. After incubation of bacteria containing solutions with the antibody, the mixture was injected over an SPR chip modified with purified-recombinant internalin B and the signal was inversely proportional to *L. monocytogenes* concentration achieving a LOD of  $2 \times 10^5$  cells/mL.

In addition to single bacteria detection, multiplexed bacteria detection with SPR systems has been also explored. Thus, an antibody microarray was developed on a SPR chip for the simultaneous detection of either *S. typhimurium*, *E. coli O157:H7*, *Yersinia enterocolitica* and *Legionella pneumophila* by modifying the chip with protein G to allow immobilization of the specific for each bacterium antibody at different areas of the chip through spotting [87]. All bacteria were detected simultaneously each at a concentration of  $10^5$  cfu/mL. *E. coli O157:H7*, *L. monocytogenes*, *Campylobacter jejuni* and *S. choleraesuis* were also simultaneously detected using a multi-channel SPR system [88]. The whole chip surface was modified with streptavidin and the four bacteria antibodies were immobilized using an 8-channel fluidic (2 channels per antibody; one for the specific and the other for the non-specific signal monitoring). The LODs achieved were  $1.4 \times 10^4$  cfu/mL for *E. coli*,  $4.4 \times 10^4$  cfu/mL for *S. choleraesuis*,  $1.1 \times 10^5$  cfu/mL for *C. jejuni*, and  $3.5 \times 10^3$  cfu/mL for *L. monocytogenes*. An SPR imaging device was combined with an array of antibodies specific against different serotypes of *L. monocytogenes* aiming to monitoring the growth of live listeria cells in culture [89]. Emphasis was given to the characterization of the antibodies rather than the analytical performance of the sensor. Similarly, the detection of *Salmonella* with an SPR imaging array was optimized and LODs of  $2.1 \times 10^6$  and  $7.6 \times 10^6$  cfu/mL, in buffer and chicken carcass rinse have been demonstrated [90]. An SPR imaging sensor has also been applied for the simultaneous label-free detection of *Salmonella* spp., Shiga-toxin producing *E. coli* (STEC) and *L. monocytogenes* in chicken carcass rinse [89]. The specific for each bacterium antibodies were immobilized on the same chip and an LOD for *Salmonella* of  $10^6$  cfu/mL was achieved. An SPR imaging sensor (Figure 6) was also implemented for the simultaneous detection of *Listeria monocytogenes* and *Listeria innocua* achieving a LOD of  $2 \times 10^2$  cfu/mL for both bacteria after 7-hour incubation of the sample in the fluidic cell attached to SPR chip [92].

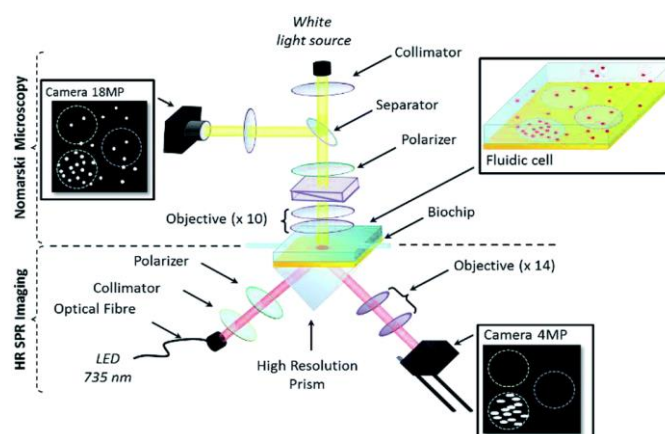


**Figure 6.** Schematic of resolution-optimized prism-based SPR imaging apparatus [92]. Copyright 2019. Reproduced with permission from the Royal Society of Chemistry.

Despite the fact that SPR has found numerous applications in diverse fields and relatively few companies have commercialized devices based on this transduction principle, the majority of these instruments are suitable for use in a lab. Thus, much effort has been devoted on reducing the equipment size and complexity in order to build up systems appropriate for analysis at the point-of-need. The SPREETA™ SPR biosensor mentioned above was a successful outcome of such an effort. It included an AlGaAs light emitting diode (LED, 840 nm), a polarizer, a temperature sensor, two

photodiode arrays, and a reflecting mirror combined with a gold-coated glass slide and a silicone rubber gasket of two channels. The instrument was accompanied by a software that provided all the information related to analysis of SPR curve, the real time binding, the layer thickness and flow cell temperatures. In addition to determination of *E. coli O157:H7* in various food samples [77], SPREETA™ SPR biosensor has been also explored for the detection of *Campylobacter jejuni* with an LOD of  $10^3$  cfu/mL [93]. SPREETA™ was also employed to develop a sensor to detect *E. coli O157:H7* in laboratory cultures [94]. The sensitivity and specificity of detection were determined. Thus, for an assay of 35 min, a LOD for *E. coli O157:H7* of  $8.7 \times 10^6$  cfu/mL was determined in single bacteria culture, whereas in mixed cultures with non-target bacteria concentrations up to  $10^6$  cfu/mL or less the LOD was  $10^7$  cfu/mL. For higher concentrations of non-target bacteria, the sensor sensitivity was negatively affected. In another report, using also the SPREETA™ SPR sensor for *E. coli* detection an LOD of 90 cfu/mL is reported for a direct binding assay that lasted less than 30 min [95]. A reason for the better performance achieved, with respect to previous reports, could be attributed to the fact that the specific antibody was immobilized onto the chip surface by streptavidin and not directly. Finally, SPREETA™ was applied to detect *Salmonella typhimurium* at concentrations equal to or higher than  $1 \times 10^6$  cfu/mL in chicken [96]. To increase the detection sensitivity of a SPREETA™ sensor for the detection of *E. coli*, Au coated magnetic nanoparticles were modified with an antibody against *E. coli* and used to concentrate *E. coli* cells from water samples but also as labels in a SPR sandwich immunoassay using SPREETA™ chips, that were modified with an anti-*E. coli* antibody, achieving a detection limit of 3 cfu/mL [97].

Apart from SPREETA™, other attempts to create portable instruments based on the SPR principle of detection have been reported in the literature. Thus, a portable instrument that combined microfluidic and SPR technologies on a single platform was applied for the determination of *E. coli* and *S. aureus* in spiked samples [98]. In this set-up an LED was used to illuminate a gold covered rectangular prism and the reflected light was captured by a CMOS sensor and then transferred for processing to a PC. The chip was modified with 11-mercaptopundecanoic acid to facilitate the covalent binding of protein G in which an antibody against the lipopolysaccharide (LPS) of *E. coli* was captured enabling *E. coli* detection at a concentration of  $3.2 \times 10^5$  cfu/mL. In another attempt, *Salmonella typhimurium* was detected in the range of  $10^7$  to  $10^9$  cfu/mL within 1 h using a SPR biosensor in which the incident light from a diode laser (instead of a LED) was directed to the gold film by a rotating mirror and the light reflected from the metal film was captured by a CMOS image sensor [99].

Another approach to surpass the portability limitations of standard SPR instruments is the implementation of localized SPR or LSPR transduction approach. In LSPR, the continuous metal surface is replaced by noble-metal nanoparticles (nanospheres, nanorods, or nanodisks) of sub-wavelength size around which the surface plasmons are localized [100]. The light that strikes the nanostructures, excites the surface plasmons and when resonance is achieved, certain wavelengths are scattered from the nanostructures. Thus, immunoreactions can be monitored in real-time as shifts in the resonance wavelength [101]. The advent of LSPR opened up new horizons for detection of pathogens, especially in the direction of portable systems. Nonetheless, the first report showed that LSPR was less sensitive than the classical SPR configuration [102] or more vulnerable to interferences from the matrix of the samples analyzed [103]. More recent reports, however, show improved detection sensitivity achieved mainly through optimization of the dimensions and stability of the nanoparticles [104]. Thus, an LSPR sensor was developed for the determination of *E. coli O157:H7* employing spherical gold nanoparticles non-covalently modified with a specific anti-*E. coli* avian antibody. A LOD of 10 cfu/mL was achieved in less than 2 h making the sensor suitable for *E. coli O157:H7* determination at the point-of-need [104]. Instead of using non-continuous gold surfaces, structuring of the gold film through its deposition onto a nanostructured fluoropolymer enabled the development of a SPR sensor based on grating-coupled long-range surface plasmons which was employed for detection of *E. coli O157:H7* through a sandwich immunoassay implementing metal nanoparticles modified with another anti-*E. coli O157:H7* antibody as labels to achieve a LOD of 50 cfu/mL [105].

The reports regarding bacteria detection with SPR based immunosensors are summarized in Table 1.

**Table 1.** SPR-based immunosensors for bacteria detection.

Analyte	Detection principle	Assay type	Sample type	Assay duration	LOD	Ref. #
<i>E. coli</i> O157:H7	SPR	sandwich	buffer	20 min	10 <sup>7</sup> cfu/mL	[63]
<i>V. cholera</i> O1	SPR	direct	buffer	-	10 <sup>5</sup> cfu/mL	[64]
<i>L. pneumophila</i>	SPR	direct	buffer	-	10 <sup>5</sup> cfu/mL	[65]
<i>E. coli</i>	SPR	direct	milk	5-7 min	23 cfu/mL	[66]
<i>S. enteritidis</i>					25 cfu/mL	
<i>S. typhimurium</i> / Enteritidis mixture	SPR	sandwich	buffer	~10 min	1.7×10 <sup>3</sup> cfu/mL	[67]
<i>S. aureus</i>	SPR	sandwich	buffer	<2 h	10 <sup>5</sup> cfu/mL	[68]
<i>E. coli</i> O157:H7	SPR	direct/ sandwich	buffer	<8 min	10 <sup>3</sup> cfu/mL	[69]
<i>S. paratyphi</i>	SPR	direct	buffer	20 min	10 <sup>2</sup> cfu/mL	[70]
<i>E. coli</i> O157:H7 Salmonella sp.	SPR	sandwich with biotinylated detection antibody and streptavidin labeled with gold nanoparticles	hamburger / cucumber	~1 h	57/17 cfu/mL 7.4×10 <sup>3</sup> /11.7×10 <sup>3</sup> cfu/mL	[71]
		direct			8×10 <sup>6</sup> cfu/mL	
<i>C. jejuni</i>	SPR	sandwich with biotinylated detection antibody and streptavidin labeled with gold	buffer	<7 min	4×10 <sup>4</sup> cfu/mL	[72]

nanoparticles						
<i>L. monocytogenes</i>	SPR	sandwich with gold-labelled secondary antibody	buffer	~35 min	10 <sup>2</sup> cfu/mL	[73]
<i>E. coli</i>	SPR	sandwich with detection antibody labeled with peroxidase + TMB substrate	fresh spinach	~2 h	10 <sup>4</sup> cfu/mL	[74]
<i>S. typhimurium</i>	SPR	direct	buffer	10 min	10 <sup>5</sup> cfu/mL	[75]
<i>E. coli O157:H7</i>	SPR	sandwich	detergent-lysed samples	50 min	10 <sup>4</sup> cfu/mL	[76]
		direct		20 min	10 <sup>6</sup> cfu/mL	
		sandwich	heat-killed samples	50 min	10 <sup>5</sup> cfu/mL	
		direct		20 min	10 <sup>7</sup> cfu/mL	
		sandwich	untreated samples	50 min	10 <sup>6</sup> cfu/mL	
		direct		20 min	10 <sup>8</sup> cfu/mL	
<i>E. coli O157:H7</i>	SPR	direct	milk apple juice ground beef	30 min	10 <sup>2</sup> -10 <sup>3</sup> cfu/mL	[77]
<i>S. typhimurium</i>	SPR	sandwich	milk	1 h	1.25x10 <sup>5</sup> cfu/mL	[78]
<i>L. monocytogenes</i>	SPR	subtractive inhibition	buffer	<30 min	10 <sup>5</sup> cells/mL	[80]
<i>E. coli O157:H7</i>	SPR	subtractive inhibition	buffer	<2 h	3.0x10 <sup>4</sup> cfu/mL	[81]
		direct		5 min	3.0x10 <sup>5</sup> cfu/mL	
<i>B. anthracis</i> spores	SPR	subtractive inhibition	buffer	40 min	10 <sup>4</sup> cfu/m	[82]

<i>Phytophthora infestans</i>	SPR	subtractive inhibition	buffer	75 min	2.2x10 <sup>6</sup> cfu/mL	[83]
<i>Puccinia striiformis</i>	SPR	subtractive inhibition	buffer	45 min	3.1x10 <sup>5</sup> cfu/mL	[84]
<i>C. parvum</i> oocysts	SPR	subtractive inhibition	water	30 min	10 <sup>2</sup> oocysts/mL	[85]
<i>L. monocytogenes</i>	SPR	inhibition	buffer chocolate milk	30 min	2x10 <sup>5</sup> cfu/mL	[86]
<i>S. typhimurium</i> <i>E. coli</i> O157:H7 <i>Yersinia enterocolitica</i> L. <i>pneumophila</i>	SPR imaging	direct	buffer	-	10 <sup>5</sup> cfu/mL	[87]
<i>L. monocytogenes</i>					3.5x10 <sup>3</sup> cfu/mL	
<i>E. coli</i> O157:H7	SPR	direct	buffer	30 min	1.4x10 <sup>4</sup> cfu/mL	[88]
<i>C. jejuni</i>	imaging		apple juice		1.1x10 <sup>5</sup> cfu/mL	
<i>S. typhimurium</i>					4.4x10 <sup>4</sup> cfu/mL	
<i>L. monocytogenes</i>	SPR imaging	direct	letuse	30 min	10 <sup>7</sup> cfu/mL	[89]
<i>S. typhimurium</i>	SPR imaging	direct	chicken carcass rinse	~20 min	7.6x10 <sup>6</sup> cfu/mL	[90]
			buffer		2.1x10 <sup>6</sup> cfu/mL	
Salmonella spp. Shiga-toxin producing <i>Escherichia coli</i>	SPR imaging	direct	chicken carcass rinse		10 <sup>6</sup> cfu/mL	[91]
<i>L. monocytogenes</i>						
<i>L. monocytogenes</i> <i>L. innocua</i>	SPR imaging	direct	buffer	7 h	2x10 <sup>2</sup> cfu/mL	[92]
<i>C. jejuni</i>	Portable SPR	direct	buffer broiler meat	<30 min	10 <sup>3</sup> cfu/mL	[93]

<i>E. coli O157:H7</i>	Portable SPR	direct	buffer	35 min	8.7×10 <sup>6</sup> cfu/mL	[94]
<i>E. coli</i>	Portable SPR	direct	water	~17 min	90 cfu/mL	[95]
<i>S. typhimurium</i>	Portable SPR	direct	chicken carcass	3 min	10 <sup>6</sup> cfu/mL	[96]
<i>E. coli</i>	SPR	direct	lake, river, puddle & tap water	20 min	3 cfu/mL	[97]
<i>E. coli</i>	Portable SPR	direct	buffer	20 min	10 <sup>6</sup> cfu/mL	[98]
<i>S. aureus</i>						
<i>S. typhimurium</i>	Portable SPR	direct	buffer	<1 h	10 <sup>7</sup> cfu/mL	[99]
<i>E. coli O157:H7</i>	LSPR	direct	buffer	80 min	10 cfu/mL	[103]
<i>E. coli O157:H7</i>	LSPR	direct	buffer	<2 h	10 cfu/mL	[104]
<i>E. coli O157:H7</i>	Portable SPR	direct	buffer	20 min	50 cfu/mL	[105]

### 3.1.2. Fiber optic immunosensors

Fiber optic immunosensors rely on immobilization of immunoreagents onto a part of the optical fiber from which the cladding layer has been removed to allow interaction of the waveguided photons through the evanescent wave field with the analyte in the solution surrounding the fiber (Figure 7). In order to increase the evanescent field effect, fiber tapering is applied either in the form of a tapered tip or of a continuous tapered fiber [45, 106]. Tapered tips are created by reducing gradually the diameter at the end of an optical fiber down to nanometers. In order to obtain the highest possible sensitivity due to reaction, the recognition biomolecules are immobilized on the tip region with the smallest diameter where the evanescent field is stronger. Continuous tapered fibers have usually a biconical taper, comprised from a region of decreasing diameter, a region of constant diameter called the waist, and a region of increasing diameter [107]. Sensing is taking place on the waist region where the evanescent field exhibits its higher intensity, whereas the emitted light is collected from the region of increasing diameter [108]. Fiber optic biosensors have been widely employed in the field of foodborne pathogen detection due to their convenience, small size, lack of electromagnetic interference, cost-effectiveness, high sensitivity and accuracy [109].

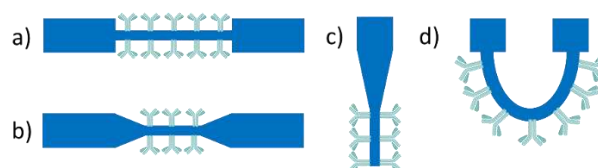


**Figure 7.** Main configurations of fiber optic sensors: (a) de-cladded optical fiber, (b) tapered optical fiber, (c) tapered tip and (d) U-shape optical fiber probe.

The first label-free approach for the detection of pathogens was realized using a U-bent optical fiber sensor [110]. Bending a de-cladded fiber into a U-shaped structure enhances the penetration depth of evanescent wave and hence sensitivity of the probe. This system could detect *E. coli* in concentrations lower than  $10^3$  cfu/mL with an assay duration of 1 h. A similar approach employing a plastic fiber optic sensor with a U-shaped sensing probe functionalized with an antibody against *E. coli* serotype O55 was employed for *E. coli* detection resulting in a LOD of  $10^3$  cfu/mL for an assay duration of 10 minutes per sample [111]. Upon exposure of the sensor to bacteria solutions, the output signal decreased with time due to the attachment of the bacteria that increased the refractive index value close to the probe.

Several fiber optic immunosensors employing labels have been also reported for bacteria detection. Thus, tapered fiber tips have been used for detection of Salmonella in culture medium [112] and *E. coli* O157:H7 in ground beef [113] with LODs of  $10^4$  and  $10^3$  cfu/mL, respectively. The first employed silica fibers with tapered tips that were modified with mercaptosilane to facilitate the covalent bonding of an anti-Salmonella antibody, while a second antibody labeled with a fluorescent dye was used as detection antibody. In the second report [113], polystyrene fibers were first coated with biotinylated bovine serum albumin and then reacted with streptavidin and biotinylated anti-*E. coli* antibody. A fluorescently labeled antibody was also used for detection. Polystyrene fibers were also integrated into a portable instrument commercialized under the name RAPTOR™. This instrument was used for the detection of *S. typhimurium* in rinse-water from sprouted alfalfa seeds through modification of the fibers first with streptavidin and then with a biotinylated antibody [114]. A second fluorescently labeled antibody was used for detection achieving a LOD of  $10^5$  cfu/mL. The RAPTOR™ biosensor has been also used to detect *Enterococcus faecalis* with a LOD of  $5.0 \times 10^5$  cells/mL [115], and *L. monocytogenes* with LODs ranging from  $10^3$  to  $4.3 \times 10^3$  cfu/mL [116-118]. In all cases, sandwich immunoassays were implemented with the exception of [117] where a fluorescently labeled aptamer (aptamer A8) specific for internalin A, an invasin protein of *L. monocytogenes*, was used for detection. A version of RAPTOR™ that supported multiplexed determinations was applied for the detection of *L. monocytogenes*, *E. coli* O157:H7 and *S. enterica* in several meat products [119]. The LOD achieved were 50 cfu/mL for *S. enterica* and  $10^3$  cfu/mL for *L. monocytogenes*.

Fluorescence resonance energy transfer, i.e., the non-radiative energy transfer from a fluorescent donor molecule to an acceptor one when these two are in close proximity, has been also implemented for detection of *S. typhimurium* with an optical fiber tip sensor in ground beef sample [120]. The anti-Salmonella antibody was labelled with the donor fluorophore (AlexaFluor 546) and protein G was labeled with the acceptor fluorophore (Alexa Fluor 594). Upon binding of *S. typhimurium* to the antibody, the induced conformation changes reduced the distance between the donor and acceptor molecules, resulting in increase of emitted fluorescence achieving an LOD of  $10^5$  cfu/g of sample.

In recent years, fiber optic immunosensors based on surface modifications with nanomaterials show significant improvements compared to conventional fiber optic sensors regarding the speed and the sensitivity of the detection. For example, a fiber optic biosensor modified with zinc oxide (ZnO) nanorods for the detection of *E. coli* in water with a LOD of  $10^3$  cfu/mL was developed [121].

Fiber optic sensors in which the exposed fiber core has been coated with a gold layer to take advantage of the SPR phenomenon have been also used for bacteria detection. Such a sensor has been employed for the detection of *Legionella pneumophila* by a direct assay after modification of the fiber gold-covered area with 11-mercaptoundecanoic to allow the covalent bonding of an anti-*L. pneumophila* antibody [122]. A LOD of 10 cfu/mL was achieved for a direct assay that lasted 1 h. In another report, a fiber optic SPR sensor was modified with MoS<sub>2</sub> nanosheets on which the specific antibodies were attached and a LOD of 94 cfu/mL for *E. coli* was achieved compared to 391 cfu/mL received from fibers without MoS<sub>2</sub> nanosheets [123]. The reports regarding bacteria detection with fiber optic based immunosensors are summarized in Table 2.

Table 2. Fiber optic sensors for bacteria detection.

Analyte	Detection principle	Assay type	Sample type	Assay duration	LOD	Ref.#
<i>E. coli</i>	fiber optic fluorescence	direct	buffer	1 h	10 <sup>3</sup> cfu/mL	[110]
<i>E. coli</i>	fiber optic	direct		10 min	10 <sup>4</sup> cfu/mL	[111]
Salmonella	fiber optic fluorescence	sandwich	buffer	1.0 h	10 <sup>4</sup> cfu/mL	[112]
<i>E. coli O157:H7</i>	fiber optic fluorescence	sandwich	ground beef	2.5 h	10 <sup>3</sup> cfu/mL	[113]
<i>S. typhimurium</i>	plastic fiber optic fluorescence	sandwich	sprouted alfalfa seeds rinse water	~30 min	10 <sup>5</sup> cfu/mL	[114]
<i>E. faecalis</i>	plastic fiber optic fluorescence	indirect	ambient water	2.5 h	10 <sup>5</sup> cfu/mL	[115]
<i>L. monocytogenes</i>	plastic fiber optic fluorescence	sandwich	buffer hot dog bologna	2.5 h	4.3x10 <sup>3</sup> cfu/mL	[116]
<i>L. monocytogenes</i>	plastic fiber optic fluorescence	sandwich	meat products	4.0 h	10 <sup>3</sup> cfu/mL	[117]
<i>L. monocytogenes</i>	plastic fiber optic fluorescence	sandwich	frankfurter	12 min	5x10 <sup>5</sup> cfu/mL	[118]
<i>L. monocytogenes</i>	plastic fiber optic		beef			
<i>E. coli O157:H7</i>	fluorescence	sandwich	chicken turkey	4.0 h	10 <sup>3</sup> cfu/mL	[119]
<i>S. enterica</i>						
<i>S. typhimurium</i>	FRET-based optical fiber	direct	buffer ground pork	5 min	10 <sup>3</sup> cells/mL 10 <sup>5</sup> cfu/g	[120]

<i>E. coli</i>	fiber optic with gold layer and ZnO nanorods	direct	water	3 s	10 <sup>3</sup> cfu/mL	[121]
<i>L. pneumophila</i>	fiber optic SPR	direct	buffer	<30 min	10 cfu/mL	[122]
<i>E. coli O157:H7</i>	fiber optic SPR	direct	drinking water	~15 min	94 cfu/mL	[123]

### 3.1.3. Interferometric immunosensors

Interferometric immunosensors is another category of devices that have been implemented for the detection of different bacteria in food matrices. These sensors could detect refractive index changes down to 10<sup>-8</sup> RIU and have demonstrated excellent analytical performance regarding the determination of analytes in complex matrices [124, 125]. The most popular configurations of interferometric sensors are Mach-Zehnder (MZI) [125-128], Young (YI) [129], Hartman [130-132] and bi-modal interferometers [133, 134].

In Mach-Zehnder interferometers, a waveguide splits into two arms, one that can detect the variations in the refractive index over its surface through a window in the cladding layer (sensing arm), and the other that is fully covered by the cladding layer and operates as reference (reference arm) [124, 125]. The two arms combine again after some point to a single waveguide and the output light intensity is monitored. Biomolecular reactions taking place onto the sensing arm window change its surface refractive index and cause a phase difference between the light beams guided in the two arms. Thus, the output light is a cosine function of the input light. This means that the sensitivity to effective refractive index changes would be maximum at the quadrature points and minimum in the vicinity of the extrema. Regarding the geometrical characteristics of the transducer, most MZIs are symmetric, i.e., the sensing and the reference arms have equal length while asymmetric MZIs, i.e., MZIs with different length of the two arms, have been also explored. The majority of MZI-based detection systems implement monochromatic light sources, i.e., lasers, which complicate instrument miniaturization and development of portable systems; therefore broad-band light sources have been explored instead of lasers. To this direction, external broad-band light sources have been coupled to MZIs integrated on the substrate [126, 127] or silicon light emitting diodes (LED) integrated onto the same silicon chip with planar silicon nitride waveguides have been implemented [125, 127]. It should be noticed that the detection sensitivities in terms of refractive index achieved with these configurations were comparable to those of MZIs implementing lasers as light sources.

A Young interferometer (YI) consists also of a waveguide divided into two arms by means of a Y-junction. The critical difference between MZIs and YIs is that in the second case, the two waveguides do not combine again but the output light interferes in air and the "interferogram" created is depicted on a CCD array. Thus, in YIs the changes in the effective refractive index over the sensing arm due to binding reactions that cause the phase difference between the two interfering beams is recorded as a shift of the interference fringes [124]. There are considerably fewer reports of integrated YIs as compared to MZIs; nonetheless, it has been demonstrated that for a particular application YI-based sensors can be more sensitive than an SPR, a grating coupler or a commercially available reflectometric interference spectroscopy (RIfS) sensor.

Hartman interferometers are based on planar waveguides in which the two modes of light, TE and TM, propagate and interact with the adlayer on the same path [124]. Changes in the refractive index cause phase shifts of the two polarizations that are not equal, because the sensitivity of the two modes to refractive index changes differs.

Bimodal interferometers are the third and most recently developed category of interferometric sensors [124]. In a bimodal interferometer the transducer is a single waveguide with two different

zones; the first supporting a single-mode and a second supporting two-modes (fundamental and first order modes). Those two modes interfere and propagate until they reach the waveguide's output. When refractive index changes occur at the waveguide surface, due to binding reactions, the interference pattern at the waveguide output also changes since the velocity with which the two modes propagate depends on the refractive index of the waveguide adlayer.

The first report for bacteria detection based on interferometric sensors was the immunochemical detection of *S. typhimurium* with a Hartman interferometer [130]. The sensor could detect  $5 \times 10^8$  cfu/mL of Salmonella in a direct assay that lasted 40 min. An integrated two-channel Hartman interferometer was also applied for the detection of *S. typhimurium* in spiked chicken rinse fluid [132]. Detection by direct binding of Salmonella cells to antibody modified waveguides was compared to a sandwich assay. Both configurations provided a LOD of  $10^4$  cfu/mL for assay duration of 10 min.

Mach-Zehnder interferometers (MZIs) have been also employed for bacteria detection. Thus, integrated onto silicon chips MZIs were modified with an antibody against *L. monocytogenes* following a chemical activation protocol specific for silicon nitride so as to limit antibody attachment to the sensing windows areas [126]. The protocol consisted of chip treatment with HF for creation of amine groups onto the silicon nitride followed by reaction with glutaraldehyde to enable covalent bonding of antibody through their free amine group. A LOD of  $10^5$  cfu/mL was achieved for a direct binding 15-min assay. In another report the MZIs waveguide was formed by patterning a photoresist layer deposited on a glass coverslip [127]. The immobilization of an antibody against *E. coli* was performed after modification of sensing arm with an aminosilane and subsequent activation with glutaraldehyde. The assay duration was 10 min and the LOD  $10^6$  cfu/mL. In another report, a chip integrating ten MZIs along with the respective silicon light emitting diodes was employed for the simultaneous detection of *S. typhimurium* and *E. coli* through a competitive immunoassay format [128]. The chip was activated with aminosilane and then the liposaccharides of *S. typhimurium* and *E. coli* were spotted onto the sensing arm windows of different MZIs of the chip and immobilized through physical adsorption. MZIs spotted with the blocking protein (bovine serum albumin) were used as reference sensors. For the assay, mixtures of calibrators or samples with the bacteria specific antibodies were run over the chip followed by reaction with biotinylated secondary antibodies and streptavidin for signal enhancement. Following this format, LODs of 40 cfu/mL for *S. typhimurium* and 110 cfu/mL in both water and milk were achieved for a 10-min assay [128].

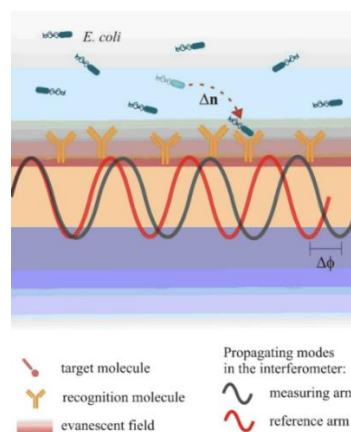


**Figure 8.** The operation of an interferometric immunosensor is based on the specific binding of the target molecule or bacteria to the antibody modified sensing arm of the interferometer. When the targeted analyte binds to the surface, a refractive index change takes place, resulting in phase difference between the propagating mode in the sensing and reference arm, leading in a light intensity change at the output [127]. Copyright 2015. Reproduced with permission from De Gruyter.

Regarding Young interferometers there are no reports for detection of bacteria, although they have been employed for the immunochemical detection of viruses, and more specifically of herpes

simplex virus type 1 (HSV-1) achieving a LOD of 850 particles/mL [129]. On the other hand, the label-free detection of *B. cereus* and *E. coli* with a bimodal interferometric immunosensor has been also reported [132]. The immobilization of antibodies was carried out either by physical adsorption of aminosilane modified chips or by covalent binding to chips modified with a carboxysilane after conversion of surface carboxyl groups to active ester groups. The device could detect 70 cfu/mL of *B. cereus* in 12.5 min and 40 cfu/mL of *E. coli* detection in 25 min. The same bimodal interferometric sensor was also applied for the detection of multidrug-resistance bacteria genes without amplification through a DNA hybridization assay [133]. Table 3 summarizes the application area and analytical performance of integrated interferometric sensors.

**Table 3.** Bacteria detection with integrated interferometric immunosensors.

Analyte	Detection principle	Assay type	Sample type	Assay duration	LOD	Ref.#
<i>S. typhimurium</i>	Hartman interferometer	direct	buffer	40 min	5x10 <sup>8</sup> cfu/mL	[130]
<i>S. typhimurium</i>	Hartman interferometer	sandwich & direct	buffer chicken carcass	10 min	10 <sup>4</sup> cfu/mL	[132]
<i>L. monocytogenes</i>	MZI fluorescence	sandwich	buffer	1.15 h	10 <sup>5</sup> cfu/mL	[126]
<i>E. coli</i>	MZI	direct	buffer	10 min	10 <sup>6</sup> cfu/mL	[127]
<i>S. typhimurium</i> <i>E. coli</i>	MZI	competitive with biotinylated secondary antibodies and streptavidin	water milk	10 min	40 cfu/mL 110 cfu/mL	[128]
<i>E. coli</i>	Bimodal interferometer	direct	buffer	25 min	40 cfu/mL	[133]
<i>B. cereus</i>				12.5 min	70 cfu/mL	

### 3.1.4. Grating coupled-based immunosensors

Grating coupler sensors are based on planar waveguides with a grating incorporated into the waveguide to enable coupling and transmission of the incident light in a manner dependent on the refractive index of the medium over the waveguide surface [42]. Thus, binding reactions that occur onto the waveguide surface can be monitored by determining the incident light in-coupling angle. In addition, since the binding reactions affect the transmitted light (through interaction with the evanescent wave field), the light out-coupling angle is also altered and can be also used to monitor the binding reactions. The second configuration is advantageous compared to the first one since there is no need for precision alignment of the light, leading thus to simpler experimental set-ups. Over the years, grating coupler sensors have been upgraded through the introduction of two-dimensional grating structures [135] or new configurations such as the wavelength interrogated optical sensor (WIOS) that implements two gratings for light in- and out-coupling to the waveguide [136] or the

angle interrogated optical sensor that uses a MEMS micro-mirror to scan the angle of the incident light of the gratings [137]. All these novel configurations allowed the development of systems for multiplexed determinations of analytes. Gratings have been also combined with other evanescent wave-based biosensors such as interferometric [138], SPR [139], SPR imaging [140], optical fiber [141], and silicon microring resonators [142], in order to create more flexible and sensitive biosensors.

A reverse symmetry waveguide sensor with an integrated grating coupler has been applied for detection of *E. coli K12* by monitoring the adhesion of bacteria cells onto the sensor surface, that has been modified with poly-L-lysine creating a protein layer with a positive charge so as to enable bacteria binding through electrostatic interactions, claiming a LOD of 60 cells/mm<sup>2</sup> [143]. Optical fiber long-period grating (LPGs) sensors have been also used for detection of *Staphylococcus aureus* through modification of the fiber surface with ionic self-assembled multilayers that facilitated the covalent bonding of antibodies specific for penicillin-binding-protein 2a of methicillin resistant staphylococci. The sensor could discriminate between methicillin-resistant and methicillin-sensitive bacteria with a LOD of 10<sup>2</sup> cfu/mL for methicillin-resistant bacteria [144]. Similarly, a long-period fiber grating sensor modified with nanopitted polyelectrolyte coatings and antibody was implemented for detection of *S. aureus* with an LOD of 224 cfu/mL for a 30-min assay [145]. Another LPG immunosensing platform formed by two identical cascaded chirped long period gratings was applied for the detection of *E. coli* [146]. The sensor worked like a Mach-Zehnder interferometer due to the space between the two gratings and could detect *E. coli* in concentrations as low as 7 cfu/mL. Finally, a grating coupler based biosensing platform known as Optical Waveguide Lightmode Spectroscopy System (OWLS), commercialized by Microvacuum Ltd. (Microvacuum Ltd.; URL: <http://www.owls-sensors.com/>), has been applied for the label-free immunochemical detection of *S. typhimurium* [147] and *L. pneumophila* [148] in water following a direct binding assay format with LODs of 1.3×10<sup>3</sup> and 1.3×10<sup>4</sup> cfu/mL, respectively. Table 4 summarizes the application area and analytical performance of grating coupler-based sensors developed for bacteria detection.

Table 4. Grating coupler-based sensors for bacteria detection.

Analyte	Detection principle	Assay type	Sample type	Assay duration	LOD	Ref.#
<i>Escherichia coli K12</i>	grating coupler	direct	buffer	1 h	1.6×10 <sup>4</sup> cfu/mL	[143]
<i>S. aureus</i>	long-period fiber gratings	direct	buffer	1 h	10 <sup>2</sup> cfu/mL	[144]
<i>S. aureus</i>	long-period fiber gratings	direct	buffer	30 min	224 cfu/mL	[145]
<i>Escherichia coli</i>	long-period fiber gratings	direct	buffer	12 min	7 cfu/ml	[144]
<i>S. typhimurium</i>	OWLS	direct	buffer	30 min	1.3×10 <sup>3</sup> cfu/mL	[147]

<i>L. pneumophila</i>	OWLS	direct	water	25 min	$1.3 \times 10^4$ cfu/mL	[148]
-----------------------	------	--------	-------	--------	-----------------------------	-------

### 3.1.5. Ring resonator-based immunosensors

Ring resonators rely on the coupling of light propagating along a linear waveguide, through the evanescent wave field, to a circular one on which propagates in the form of whispering-gallery modes. Any change in the refractive index in the proximity of the ring surface affects the spectral position of the whispering-gallery modes and changes the wavelength of the incident light for which resonance is achieved. As the light propagating in the ring can interact multiple times with the molecules on its surface, ring resonators are expected to provide the same performance (denoted by the Q factor) with that obtained from linear waveguides with many times longer length. Thus, by implementing ring resonators as transducers, smaller size devices as compared to linear waveguides and denser transducer arrays can be realized. Ring resonators can adopt the 2D format of a microdisk [149] or microring [150], but also the 3D format of a microtoroid [151]. Toroids are claiming higher Q factors than the planar resonators and therefore, higher detection sensitivity is expected. Sensors based on microring resonators have been also explored with regard to bacteria detection. Detection of *E. coli* with a microring resonator sensor has been reported and the relatively high LOD of  $10^5$  cfu/mL was ascribed to suboptimal functionalization of resonators with bacteria-binding antibodies (Figure 9) [152].

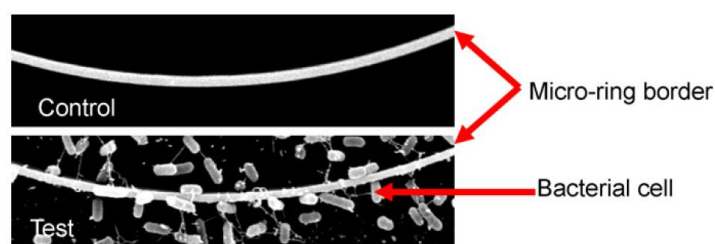


**Figure 9.** Scanning electron micrographs of a small section of test and control micro-rings on a resonator chip, showing specific bacterial binding at 2200x magnification [152]. Copyright 2007. Reproduced with permission from Elsevier B.V.

Finally, a whispering gallery mode optical microdisk resonator was modified with the phage protein LysK, an endolysin from the staphylococcal phage K that binds strongly to staphylococci and used to detect *S. aureus* with a LOD of  $5 \times 10^6$  cfu/mL [153].

### 3.2. Reflectometric immunosensors

Reflectometric sensors rely on monitoring shifts in the interference spectrum due to binding reactions taking place on a stack of materials with different refractive indices. The illumination sources usually employed are white light sources.

A commercially available RIfS-based biosensing device was used to detect *L. pneumophila* by monitoring either the direct capture of bacteria cells via electrostatic interaction onto the chip surface or through a sandwich assay [154]. The device performance was compared to that of SPR and a LOD of  $1 \times 10^5$  cfu/mL was determined in both cases. A white light reflectance spectroscopy based immunosensor exhibited a better performance regarding the rapid and sensitive detection of *S. typhimurium* in drinking water (Figure 10) [155]. The sensor chip consisted of a Si die with a thin SiO<sub>2</sub> layer on top and *S. typhimurium* detection was performed through a competitive immunoassay format between bacteria in the sample and the immobilized onto chip Salmonella liposaccharide. A LOD of 320 cfu/mL was achieved for an assay duration of 15 min.

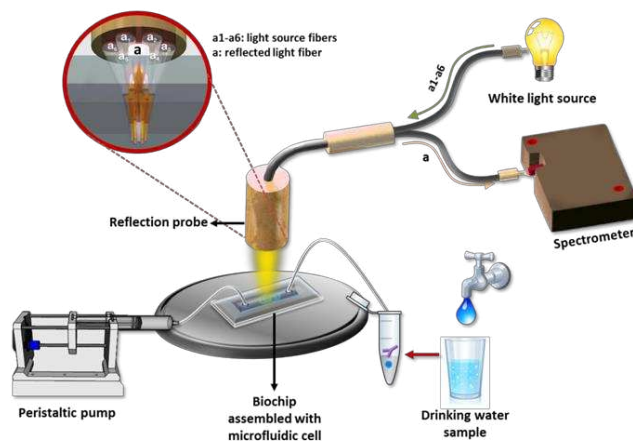


**Figure 10.** Illustration of the white light reflectance spectroscopy (WLRS) optical setup and sensing principle [155]. Copyright 2021. Reproduced with permission from MDPI.

Porous silicon has been also employed as substrate for detection of bacteria through Reflectance spectroscopy. Thus, the label-free detection of *E. coli* K12 was achieved using a sensor based on a nanostructured oxidized porous silicon thin film [156, 157]. The sensor surface was functionalized with specific antibodies against *E. coli* through aminosilanization and activation of surface amine groups with bis(*N*-succinimidyl)carbonate for coupling of antibodies via their free amine groups [156, 157]. The LOD determined was about  $10^4$  cells/mL and the assay was completed in 30 min. An optimization of the same sensor, in which a different surface modification was followed (Figure 11), resulted in a LOD of  $10^3$  cells/mL in water for an assay of 45 min [158]. In this case, after aminosilanization, the surface was functionalized with glutaraldehyde to introduce aldehyde groups through which streptavidin was bound onto the surface to facilitate immobilization of biotinylated anti-bacteria specific antibodies.

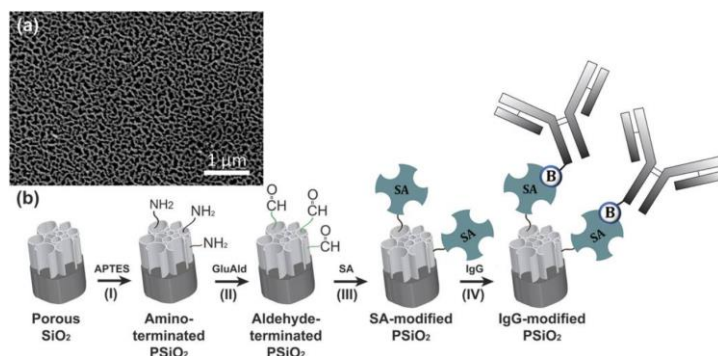


**Figure 11.** (a) A top-view high-resolution scanning electron microscope image of a typical PSiO<sub>2</sub> film with typical pores in the range of 60–100 nm. (b) Schematic representation of the steps followed to bio-functionalize the PSiO<sub>2</sub> surface with IgG, including: (I) 3-aminopropyl-triethoxysilane modification, (II) reaction of amine-terminated PSiO<sub>2</sub> with one of the aldehyde groups of the cross-linker glutaraldehyde, (III) grafting of streptavidin onto the aldehyde-terminated surface, (IV) conjugation of biotinylated-IgG (*E. coli*) via biotin-streptavidin binding [158]. Copyright 2016. Reproduced with permission from Springer Nature.

Another biosensor developed for bacteria detection on porous silicon substrates involved surface modification with a hydrogel made of polyacrylamide to which biotinylated specific monoclonal antibodies were immobilized onto streptavidin covalently bound to surface after appropriate chemical functionalization [159]. A detection limit in the range of  $10^3$ – $10^5$  cell/mL was determined for direct bacteria binding for 30 min. Furthermore, for the direct detection of *E. coli*, a

biosensor based on blockage of nanopores created by etching of Si chip was presented achieving a detection limit of  $10^3$  cfu/mL [160]. More specifically, when *E. coli* cells were trapped into the chip nanopores, a decrease of effective optical thickness was recorded. Thus, by monitoring the change of effective optical thickness value, it was possible to quantitatively determine the cells captured in the nanopores via indirect Fourier Transformed Reflectometric Interference Spectroscopy.

Finally, an interferometric reflectance imaging system was employed for the label-free detection of *E. coli* [161]. The bacteria specific antibody was spotted onto a SiO<sub>2</sub>/Si chip modified with a polymer and after incubation for 2 h with the bacteria solutions the bound cells were counted using a low-magnification optical set-up accompanied by an appropriate software. Based on experimental data, an extrapolated LOD of 2.2 cfu/mL was calculated which is the lowest, so far, reported for direct bacteria detection.

**Table 5.** Bacteria detection with reflectometric immunosensors.

Analyte	Detection principle	Assay type	Sample type	Assay duration	LOD	Ref.#
<i>L. pneumophila</i>	RIfS	direct	buffer	30 min	$1 \times 10^5$ cfu/mL	[154]
		sandwich		60 min		
<i>S. typhimurium</i>	WLRS	competitive	drinking water	15 min	320 cfu/mL	[155]
<i>E. coli K12</i>	reflectance spectroscopy on porous silicon	direct	buffer	30 min	$10^4$ cells/mL	[156]
<i>E. coli</i>	reflectance spectroscopy on porous silicon	direct	buffer	30 min	$10^4$ cells/ml	[157]
<i>E. coli</i>	reflectance spectroscopy on porous silicon	direct	water	45 min	$10^3$ cells/mL	[158]
<i>E. coli</i>	reflectance spectroscopy on porous silicon	direct	buffer	30 min	$10^3$ cells/mL	[159]
<i>E. coli</i>	Fourier Transformed Reflectometric Interference Spectroscopy	direct	buffer	40 min	$10^3$ cfu/mL	[160]
<i>E. coli</i>	reflectance spectroscopy	direct	tap water	2 h	2.2 cfu/mL	[161]

## imaging

## 3.4. Photoluminescence-based immunosensors

Photoluminescence (fluorescence and phosphorescence) is the phenomenon of light emission from a molecule that has been excited by adsorption of photons in the visible or UV region [162]. An optical immunosensor based on glass slides modified with TiO<sub>2</sub> nanoparticles was developed exploiting the decrease in photoluminescence intensity of TiO<sub>2</sub> nanoparticles modified with antibodies against *S. typhimurium* upon binding of bacteria from solutions with concentration in the range 10<sup>3</sup> to 10<sup>5</sup> cells/mL [163]. A fluorescent array biosensor prepared on soda lime glass substrate, which was employed as waveguide, was used for the detection of *S. typhimurium* through a sandwich immunoassay with fluorescently labeled antibodies. The LOD was 8×10<sup>4</sup> cfu/mL and the assay duration 15 min [164]. This array biosensor was used to detect *Shigella dysenteriae* in buffer and chicken carcass wash and *Campylobacter jejuni* at concentrations as low as 4.9×10<sup>4</sup> and 9.7×10<sup>2</sup> cfu/mL, respectively, by applying sandwich immunoassays that lasted 25 min [165]. The same sensor was applied to detect the bacterium *Campylobacter jejuni* following a 25-min sandwich immunoassay in a number of different food matrices with a LOD of 500 cells/mL [166]. Finally, the sensor was applied to detect *Escherichia coli* in less than 30 min in various spiked food matrices with LODs in the range 1-5×10<sup>4</sup> cells/mL [167].

A homogeneous FRET immunosensor using antibodies conjugated to graphene oxide quantum dots and graphene oxide sheets was designed for detection of *C. jejuni* cells in food samples [168]. The graphene oxide quantum dots conjugated antibody interacted with the graphene oxide sheets through a π-π stacking leading to fluorescence quenching. When *C. jejuni* was selectively captured by the antibody, this interaction was disrupted and the fluorescence emission increased proportionally to concentration of bacteria in the sample. The assay was completed in 1.5 h and the LOD was 10 cfu/mL.

Table 6. Photoluminescence-based immunosensors for bacteria detection.

Analyte	Detection principle	Assay type	Sample type	Assay duration	LOD	Ref.#
<i>S. typhimurium</i>	label-free	direct	buffer	<30 min	10 <sup>3</sup> cells/mL	[163]
<i>S. typhimurium</i>	fluorescence	sandwich	Poultry chicken excretal samples	15 min	8×10 <sup>4</sup> cfu/mL	[164]
<i>Shigella dysenteriae</i> <i>C. jejuni</i>	fluorescence	sandwich	buffer and chicken carcass	25 min	4.9×10 <sup>4</sup> cfu/mL 9.7×10 <sup>2</sup> cfu/mL	[165]
<i>C. jejuni</i>	fluorescence	sandwich	ground turkey sausage & ham carnation nonfat dried milk	25 min	500 cells/mL	[166]

			vanilla fat free yogurt			
			ground beef			
<i>Escherichia coli</i>	fluorescence	sandwich	turkey sausage carcass wash	30 min	1-5×10 <sup>4</sup> cells/mL	[167]
			apple juice			
<i>C. jejuni</i>	homogeneous FRET	direct	poultry liver	1.5 h	10 cfu/mL	[168]

### 3.5. Surface Enhanced Raman Scattering (SERS) -based immunosensors

SERS-based biosensors combine the Raman inelastic scattering phenomenon of incident laser light with signal enhancement provided from nanostructured noble metal substrates [169]. More specifically, the Raman signal of molecules adsorbed onto the SERS surfaces is enhanced by a factor of 10<sup>4</sup>–10<sup>8</sup> due to the strong electromagnetic field generated on the surface of these substrates. This enhanced scattering phenomenon results in characteristic peaks due to the vibrational modes of the molecules, which provide a fingerprint unique to each molecule. Thus, in SERS-based bioanalysis, the target molecules can either be detected directly after their attachment to the nanostructured surfaces (Figure 12a), through their binding to surface-anchored recognition elements, such as antibodies (Figure 12b) and through sandwich immunoassays employing SERS-active labels for signal enhancement (Figure 12c) [170-173]. SERS active labels or tags are prepared by conjugating the analyte-specific antibodies to nanoparticles along with Raman reporter molecules, which are low-molecular weight moieties with strong and distinguishable Raman signals. All these approaches have been implemented for bacteria detection through SERS.

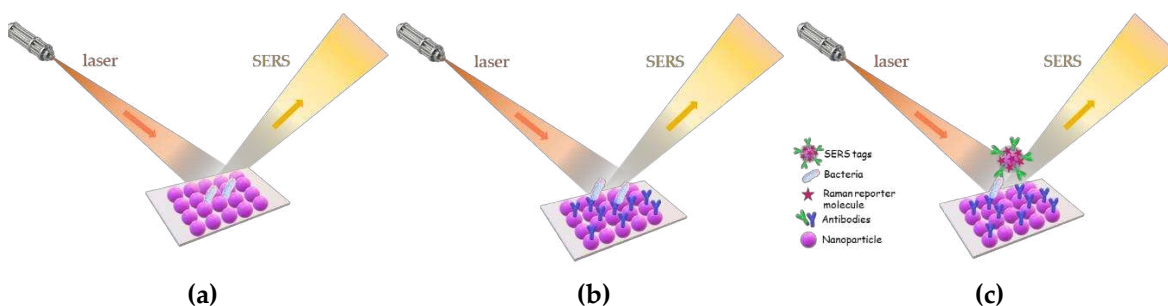


**Figure 12.** Schematic illustration of SERS-based approaches for (a) direct, (b) immunochemical, or (c) label-based detection with SERS tags.

Knauer et al. developed direct label-free SERS-based immunochemical methods for the detection of *L. pneumophila* and *S. typhimurium* in a single run [174], and of *E. coli* [175] as well. Regarding the simultaneous determination of *S. typhimurium* and *L. pneumophila*, glass substrates were modified with an epoxy-silane and then reacted with a diamine-polyethylene glycol to introduce amine groups onto the surfaces, which are then implemented for the covalent bonding of antibodies specific against the two bacteria by spotting at different areas of the substrate. After bacteria binding, the surfaces were incubated with an Ag colloid preparation that aggregated onto the immobilized bacteria creating “hot spots” which provided strong Raman signal. The assay lasted 65 min and the LODs achieved were 10<sup>6</sup> and 10<sup>8</sup> cells/mL for *L. pneumophila* and *S. typhimurium*, respectively [174]. For *E. coli* detection, the antibody modified substrates were combined with a flow-through system enabling detection of *E. coli* strains in concentrations down to 4.3×10<sup>3</sup> cfu/mL in water samples of 100 mL [175]. A LOD of 10 cfu/mL was achieved for *E. coli* O157:H7 when a SERS-based non-competitive

immunoassay using a combination of antibody-modified magnetic particles and gold nanoparticles modified with an anti-bacterium antibody and a SERS tag molecule [176]. At first the bacteria solution was incubated with the antibody-labelled magnetic nanoparticles and after magnetic separation they were incubated with the SERS-tagged antibody-modified gold nanoparticles. The immunocomplexes formed were separated from free antibodies using a membrane filter on which the Raman was determined [176]. A similar immunoassay format was applied to the simultaneous detection of *E. coli* O157:H7 and *S. aureus* with LODs of 10 and 25 cfu/mL, respectively [177]. In this case, magnetic beads and SERS active gold nanoparticles functionalized with specific antibody pairs against each bacterium were used and the simultaneous determination was based on the use of a different SERS tag for each bacterium. After formation of immunocomplexes in liquid phase, a magnetic field was applied and the Raman signals from the two different tags quantified [177]. In another report, the capture antibodies were immobilized on magnetite-gold nanoparticles to enable separation and concentration of the *E. coli* O157 cells from the liquid, and then were reacted with gold nanoparticles modified with antibodies and Raman tags [178]. This method provided rapid separation and detection (less than one hour) of *E. coli* achieving a LOD of  $10^2$  cfu/mL. A similar approach was applied for the isolation and detection of multiple pathogenic bacteria through the implementation of lectin functionalized silver coated magnetic nanoparticles to bind and separate bacteria prior to reaction with SERS-tagged silver nanoparticles functionalized with antibodies specific for each one of the targeted bacteria. Thus, *E. coli*, *S. typhimurium*, and methicillin-resistant *S. aureus* isolation and detection were achieved at concentrations as low as 10 cfu/mL [179]. Gold-coated magnetic nanoparticles (gold coated  $\text{MnFe}_2\text{O}_4$  nanoparticles) were conjugated with antibodies against *S. aureus* and used as SERS tags as well as for bacteria capture and separation resulting in an assay with LOD of 10 cfu/mL [180]. Spherical and rod-shaped gold nanoparticles modified with Raman tags and an antibody against *E. coli* were compared as labels in a sandwich immunoassay with capture antibody immobilized onto a gold-coated glass slide [181]. The LODs determined using the gold nanorods and the spherical gold nanoparticles as labels were 4 and 5 cfu/mL, respectively. Rod-shaped gold covered magnetic nanoparticles modified with an antibody against *E. coli* have been also investigated as labels in a liquid phase assay for detection of *E. coli* at concentrations as low as LOD 35 cfu/mL [182]. The difference in the LOD of this report compared to the previous one that used the same label [181] was attributed to lower capture efficiency of magnetic gold nanorod particles as compared to the gold-coated glass slide surface. Thus, when the same group implemented gold-coated magnetic spherical nanoparticles modified with an anti-*E. coli* antibody in combination with rod shaped gold nanoparticles modified with Raman tags and an anti-*E. coli* antibody, a LOD of 8 cfu/mL was achieved [183]. In another detection approach, SERS was combined with a microfluidic dielectrophoresis device to detect *Salmonella enterica* serotype Choleraesuis and *Neisseria lactamica* [184]. The SERS labels employed were silica-coated dye-induced aggregates of a small number of gold nanoparticles, denoted as nanoaggregate-embedded beads, and were modified with antibodies specific for each bacterium to allow their online detection with an LOD of 70 cfu/mL. SERS detection was also combined with lateral flow strip biosensors. Thus, *L. monocytogenes* and *S. typhimurium* were simultaneously detected with a lateral flow sandwich immunoassay employing gold nanoparticles modified with a Raman tag and specific antibodies against each one of the targeted bacteria [185]. The LODs achieved were 75 cfu/mL for both bacteria and the strip assay was applied for bacteria detection in milk samples. Another lateral flow strip biosensor employing SERS labels combined with recombinase polymerase amplification (RPA) was applied for the simultaneous determination of *S. enteritidis* and *L. monocytogenes* [186]. The method made use of forward primers labeled with digoxin and fluorescein for *S. enteritidis* and *L. monocytogenes*, respectively, whereas the reverse primers were labeled with biotin. Thus, when the RPA product was applied to the sample pad, it was run along with gold nanoparticles modified with streptavidin and Raman tags towards the two test lines where antibodies against digitoxin and fluorescein have been spotted, resulting in the creation of the respective colored lines (Figure 13). The LODs achieved were 27 and 19 cfu/mL for *S. enteritidis* and

*L. monocytogenes*, respectively [186]. The same approach was employed to detect *Escherichia coli* O157:H7 with an LOD of  $5 \times 10^4$  cfu/mL in milk, chicken breast, and beef [187].

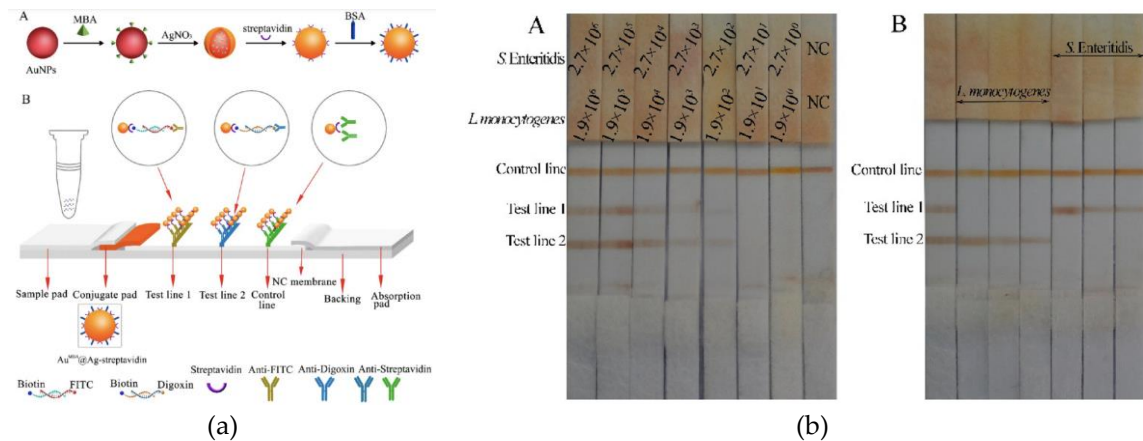


**Figure 13.** a) Schematic illustration of: (A) preparation of gold nanoparticles modified with streptavidin and Raman tags (MBA), and (B) the multiplex lateral flow SERS assay. b) (A) Results from lateral flow strips for the simultaneous detection of *S. enteritidis* (test line 1) and *L. monocytogenes* (test line 2). Test lines could be observed by naked eye at a concentration of  $1.9 \times 10^2$  cfu/mL of *L. monocytogenes* and  $2.7 \times 10^2$  cfu/mL of *S. Enteritidis*. The SERS signal of the test lines could be detected at a concentration of  $1.9 \times 10^1$  cfu/mL of *L. monocytogenes* and  $2.7 \times 10^1$  cfu/mL of *S. Enteritidis*. (B) Specificity of the lateral flow strip assay against three *L. monocytogenes* and three *S. enteritidis* bacteria [186]. Copyright 2017. Reproduced with permission from the American Chemical Society.

In Table 7 the data regarding bacteria detection with SERS-based biosensors are presented.

**Table 7.** SERS-based immunosensors for bacteria detection.

Analyte	Detection principle	Assay type	Sample type	Assay duration	LOD	Ref.#
<i>L. pneumophila</i> <i>S. typhimurium</i>	SERS	direct	water	65 min	$10^6$ cfu/mL $10^8$ cfu/mL	[174]
<i>E. coli</i> O157:H7	SERS	direct	water	>60 min	$4.3 \times 10^3$ cfu/mL	[175]
<i>E. coli</i> O157:H7	SERS	sandwich	ground beef	~2 h	10 cfu/mL	[176]
<i>E. coli</i> <i>S. aureus</i>	SERS	sandwich	bottled water milk	~2h	10 cfu/mL 25 cfu/mL	[177]
<i>E. coli</i> O157	SERS	sandwich	apple juice	<1 h	$10^2$ cfu/mL	[178]
<i>E. coli</i> <i>S. typhimurium</i> methicillin-resistant	SERS	sandwich	buffer	>30 min	10 cfu/mL	[179]

<i>S. aureus</i>						
<i>S. aureus</i>	SERS	sandwich	buffer	-	10 cells/mL	[180]
<i>E. coli</i> K12	SERS	sandwich	buffer	<2 h	4 cfu/mL	[181]
<i>E. coli</i>	SERS	sandwich	buffer	70 min	35 cfu/mL	[182]
<i>E. coli</i>	SERS	sandwich	water	70 min	8 cfu/mL	[183]
Salmonella <i>enterica</i> serotype <i>Choleraesuis</i>						
	SERS	direct	buffer	<2 h	70 cfu/mL	[184]
Neisseria <i>lactamica</i>						
L. <i>monocytogenes</i>						
	LFIA SERS	sandwich	milk	10 min	75 cfu/mL	[185]
<i>S. typhimurium</i>						
<i>S. enteritidis</i> /						
L. <i>monocytogenes</i>	LFIA SERS	sandwich	buffer chicken breast beef milk	30 min	27/19 cfu/mL 35/29 cfu/mL 35/22 cfu/mL 31/36 cfu/mL	[186]
<i>E. coli</i> O157:H7						
	LFIA SERS	sandwich	milk chicken breast beef	15 min	5x10 <sup>4</sup> cfu/mL	[187]

#### 4. Conclusions and outlook

This review has outlined the principles and applications of antibody-based optical sensors in the detection of food pathogenic bacteria. Although there is an abundance of relative publications, there seems that very few of the available sensing principles have been exploited for the detection of bacteria in real food samples. Thus, although fiber optic sensors employing fluorescent labels have been the first to be implemented for bacteria detection in food samples, the great majority of references, especially the most recent ones, rely on SPR sensors. The reason for that relies probably on the availability of different instruments based on the SPR detection principle, some of which are commercially available. Nevertheless, the LODs achieved in most of the cases ranged from 10<sup>3</sup>-10<sup>5</sup> cfu/mL, which are considered high for direct application to food analysis and they should be combined with a sample enrichment procedure that adds a few hours to the total time required from sampling to answer. There are a few reports however that report LODs of a few or a few tens of cfu/mL [66, 95, 97, 103-105], from which only one is performed in a standard benchtop SPR instrument [66], and two others with a commercially available portable SPR instrument (SPREETA™) [95, 97], which is not currently in the market. The first two reports were based on direct binding

assays for label-free detection of targeted bacteria [66, 95], whereas in the third, gold magnetic particles were employed as labels to drop the LOD to 3 cfu/mL [97]. The rest of the reports implement the localized SPR (LSPR) principle either in the form of gold nanoparticles [103, 104] or in the form of nanostructured gold film [105]. In addition to higher detection sensitivity, LSPR is also considered more easily adaptative to portable low-cost devices and it remains to be seen what would be done to this direction in the near future. Regarding the majority of fiber optic based immunosensors the LODs achieved for bacteria detection also ranged from  $10^3$ - $10^5$  cfu/mL. LODs of less than 100 cfu/mL were achieved only when fibers were combined with SPR via covering their sensing area with a gold film or gold nanoparticles or films of other materials (e.g., MoS<sub>2</sub> nanosheets) [122, 123]. Since, fiber optic experimental set-up can be also reduced in size and cost, the combination with SPR might also be proved a viable solution for portable devices in the future. Integrated interferometers, particularly in the form of MZIs [128] and bimodal interferometers [133] have shown adequate sensitivity for bacteria detection (LODs in the range of a few tens of cfu/mL) combined with short assay times and great potential for multiplexed determinations. There seem also to be the most promising candidate to the direction of portable devices suitable for point-of-need determinations. On the other hand, microring resonators or microtoroids, despite their claimed high detection sensitivity, are the optical transducers less frequently employed for bacteria detection, whereas the few reports existing present LODs non competitive to other types of optical biosensors [152, 153]. The same seems to be true for most of the immunosensors based on grating couplers for which there is only one report with a LOD of a few cfu/mL in which an optical fiber grating device has been implemented [144]. Immunosensors based on reflectance spectroscopy have also demonstrate the potential for detection of bacteria at concentrations as low as 2.2 cfu/mL [161], whereas, the assay was performed in a 24-well plate with the IRIS chip placed at the bottom of each well and lasted over 2 h. A more compact system based on reflectance spectroscopy achieved an LOD of 320 cfu/mL with a 15-min assay, allowing the detection of bacteria in food samples after a short pre-enrichment step (3-4 h) [155]. The most impressive performance regarding the percentage of reports that mention LODs of less than 100 cfu/mL present the immunosensors based on SERS [176-182, 184-186]. However, with the exception of two reports where Raman spectroscopy is combined with a lateral flow immunoassay [182, 184] for which the assay duration was less than 30 min, most sensors required more than 1 h to complete the assay.

Regarding the assay type implemented for bacteria detection with optical immunosensors, although direct binding onto antibody-modified transducers has been widely used, it has been rarely led to high detection sensitivity combined with short assay time. Thus, competitive or non-competitive immunoassay formats have been employed to increase detection sensitivity and/or decrease assay duration. This might complicate a bit the development of portable devices since it requires the integration of optical sensors with microfluidic modules, pumps and valves which will provide for the automated execution of the assay steps. In addition, this integration should be performed in such a way that it will not increase either the device size or the cost.

To the direction of developing portable devices based on optical transducers, the tools offered by the continuously evolving smartphone gadgets, either as light sources or for the detection of optical signal or the ability to run the instrument software in such a device, process the data, and transfer them wirelessly to central facilities, are considered a significant asset.

Although, the current technological limitations are more than certain that they will be surpassed in the near future, there are some aspects of optical immunosensors that need to further addressed prior to their application for bacteria detection at the point-of-need. For example, the study of relevant literature reveals that the sensitive bacteria detection with immunochemical techniques is often challenging due to lack of appropriate antibodies. Thus, in many instances, optical immunosensors have been developed using in-house produced antibodies that are not widely available. Even, if antibodies with appropriate binding characteristics for the specific and sensitive detection of a particular bacterium are commercially available, their suitability for detection of bacteria in processed foods has to be investigated since the structure of bacteria epitopes could change dramatically when

the food has been processed at certain conditions of temperature or pH. In addition, in many instances antibodies cannot discriminate viable from non-viable cells providing false positive results.

Despite the above-mentioned limitations of optical immunosensors for bacteria detection, they remain one of our best hopes for sensitive portable devices that would be available at affordable prices with low operation costs so as to find wide application in food industry, retailers, and food-safety control departments in order to ensure the safety of our food.

**Author Contributions:** Conceptualization, D.K. and M.A.; writing—original draft preparation, D.K., M.A. and P.P.; writing—review and editing, M.A., P.P. and S.K.; funding acquisition, M.A., P.P. and S.K. All authors have read and agreed to the published version of the manuscript.

**Funding:** This research has been co-financed by the European Regional Development Fund of the European Union and Greek national funds through the Operational Program Competitiveness, Entrepreneurship and Innovation, under the call RESEARCH–CREATE–INNOVATE (project code: T2EΔK-01934/FOODSENS), and European Union’s Horizon 2020 Research and Innovation program through the Marie Skłodowska-Curie grant agreement No 101007299 (SAFEMILK).

**Institutional Review Board Statement:** Not applicable.

**Data Availability Statement:** No new data were created or analyzed in this study. Data sharing is not applicable to this article.

**Conflicts of Interest:** The authors declare no conflict of interest.

## References

1. World Health Organization. Foodborne Diseases. Available online: [https://www.who.int/health-topics/foodborne-diseases#tab=tab\\_1](https://www.who.int/health-topics/foodborne-diseases#tab=tab_1) (accessed on 18/06/2023)
2. World Health Organization. The Top 10 Causes of Death. Available online: <https://www.who.int/news-room/fact-sheets/detail/the-top-10-causes-of-death> (accessed on 18/06/2023)
3. World Health Organization. Estimating the Burden of Foodborne Diseases: A Practical Handbook for Countries. World Health Organization, Geneva, 2021.
4. Addis, M.; Sisay, D. A review on major food borne bacterial illnesses. *J. Trop. Dis.* **2015**, *3*, 1000176.
5. Madigan, M.; Martinko, J.; Stahl, D.; Clark, D.P. *Brock Biology of Microorganisms*, 13th ed.; Benjamin Cummings, CA, USA, 2012; pp. 1022–1042.
6. Zourob, M.; Elwary, S.; Turner, A. *Principles of Bacterial Detection: Biosensors, Recognition receptors and Microsystems*, 1st ed.; Springer Science+Business Media, LLC: NY, USA, 2008.
7. Saravanan, A.; Kumar, P.S.; Hemavathy, R.V.; Jeevanantham, S.; Kamalesh, R.; Sneha, S.; Yaashikaa, P.R. Methods of detection of food-borne pathogens: A review. *Environ. Chem. Lett.* **2021**, *19*, 189–207.
8. Gracias, K.S.; McKillip, J.L. A review of conventional detection and enumeration methods for pathogenic bacteria in food. *Can. J. Microbiol.* **2004**, *50*, 883–890.
9. Zhao, X.; Lin, C.W.; Wang, J.; Oh, D.H. Advances in rapid detection methods for foodborne pathogens. *J. Microbiol. Biotechnol.* **2014**, *24*, 297–312.
10. Wang, Y.; Salazar, J.K. Culture-independent rapid detection methods for bacterial pathogens and toxins in food matrices. *Compr. Rev. Food Sci. Food Safety* **2016**, *15*, 183–205.
11. Garrido-Maestu, A.; Tomás Fornés, D.; Prado Rodríguez, M. The use of multiplex real-time PCR for the simultaneous detection of foodborne bacterial pathogens. In *Foodborne Bacterial Pathogens: Methods and Protocols*. Bridier A. Ed., Springer Science+Business Media, LLC: NY, USA, 2019; Volume 1918, pp. 35–45.
12. Lee, N.; Kwon, K.Y.; Oh, S.K.; Chang, H.J.; Chun, H.S.; Choi, S.W. A multiplex PCR assay for simultaneous detection of *Escherichia coli* O157:H7, *Bacillus cereus*, *Vibrio parahaemolyticus*, *Salmonella* spp., *Listeria monocytogenes*, and *Staphylococcus aureus* in Korean ready-to-eat food. *Foodborne Pathog. Dis.* **2014**, *11*, 574–580.
13. Liu, Y.; Cao, Y.; Wang, T.; Dong, Q.; Li, J.; Niu, C. Detection of 12 common food-borne bacterial pathogens by Taq Man real-time PCR using a single set of reaction conditions. *Front. Microbiol.* **2019**, *10*, 222.
14. Magliulo, M.; Simoni, P.; Guardigli, M.; Michelini, E.; Luciani, M.; Lelli, R.; Roda, A. A rapid multiplexed chemiluminescent immunoassay for the detection of *Escherichia coli* O157:H7, *Yersinia enterocolitica*, *Salmonella typhimurium*, and *Listeria monocytogenes* pathogen bacteria. *J. Agric. Food Chem.* **2007**, *55*, 4933–4939.

15. Cavaiuolo, M.; Paramithiotis, S.; Drosinos, E.H.; Ferrante, A. Development and optimization of an ELISA based method to detect *Listeria monocytogenes* and *Escherichia coli* O157 in fresh vegetables. *Anal. Methods* **2013**, *5*, 4622–4627.
16. Zhu, L.; He, J.; Cao, X.; Huang, K.; Luo, Y.; Xu, W. Development of a double-antibody sandwich ELISA for rapid detection of *Bacillus cereus* in food. *Sci. Rep.* **2016**, *6*, 16092.
17. Hochel, I.; Slavíčková, D.; Viochna, D.; Škvor, J.; Steinhauserová, I. Detection of *Campylobacter* species in foods by indirect competitive ELISA using hen and rabbit antibodies. *Food Agric. Immunol.* **2007**, *18*, 151–167.
18. Rohde, A.; Hammerl, J.A.; Boone, I.; Jansen, W.; Fohler, S.; Klein, G.; Dieckmann, R.; Al Dahouk, S. Overview of validated alternative methods for the detection of foodborne bacterial pathogens. *Trend Food Sci. Technol.* **2017**, *62*, 113–118.
19. Law, J.W.F.; Mutalib, N.S.A.; Chan, K.G.; Lee, L.H. Rapid methods for the detection of foodborne bacterial pathogens: Principles, applications, advantages and limitations. *Front. Microbiol.* **2014**, *5*, 770.
20. Khansili, N.; Rattu, G.; Krishna, P.M. Label-free optical biosensors for food and biological sensor applications. *Sens. Actuator B* **2018**, *265*, 35–49.
21. Qiao, Z.; Fu, Y.; Lei, C.; Li, Y. Advances in antimicrobial peptides-based biosensing methods for detection of foodborne pathogens: A review. *Food Control* **2020**, *112*, 107116.
22. Thévenot, D.R.; Toth, K.; Durst, R.A.; Wilson, G.S. Electrochemical biosensors: Recommended definitions and classification. *Biosens. Bioelectron.* **2001**, *16*, 121–131.
23. Morales, M.A.; Halpern, J.M. Guide to selecting a biorecognition element for biosensors. *Bioconjugate Chem.* **2018**, *29*, 3231–3239.
24. Wu, Q.; Zhang, Y.; Yang, Q.; Yuan, N.; Zhang, W. Review of electrochemical DNA biosensors for detecting food borne pathogens. *Sensors* **2019**, *19*, 4916.
25. Ansari, N.; Yazdian-Robati, R.; Shahdordizadeh, M.; Wang, Z.; Ghazvini, K. Aptasensors for quantitative detection of *Salmonella typhimurium*. *Anal. Biochem.* **2017**, *533*, 18–25.
26. Tawil, N.; Sacher, E.; Mandeville, R.; Meunier, M. Surface plasmon resonance detection of *E. coli* and methicillin-resistant *S. aureus* using bacteriophages. *Biosens. Bioelectron.* **2012**, *37*, 24–29.
27. Wen, T.; Wang, R.; Sotero, A.; Li, Y. A portable impedance immunosensing system for rapid detection of *Salmonella typhimurium*. *Sensors* **2017**, *17*, 1973.
28. Viswanathan, S.; Rani, C.; Ho, J.A.A. Electrochemical immunosensor for multiplexed detection of foodborne pathogens using nanocrystal bioconjugates and MWCNT screen-printed electrode. *Talanta* **2012**, *94*, 315–319.
29. Fulgione, A.; Cimafonte, M.; Della Ventura, B.; Iannaccone, M.; Ambrosino, C.; Capuano, F.; Proroga, Y.T.R.; Velotta, R.; Capparelli, R. QCM-based immunosensor for rapid detection of *Salmonella typhimurium* in food. *Sci. Rep.* **2018**, *8*, 16137.
30. Ye, Y.; Guo, H.; Sun, X. Recent progress on cell-based biosensors for analysis of food safety and quality control. *Biosens. Bioelectron.* **2019**, *126*, 389–404.
31. Templier, V.; Roux, A.; Roupioz, Y.; Livache, T. Ligands for label-free detection of whole bacteria on biosensors: A review. *TrAC – Trend Anal. Chem.* **2016**, *79*, 71–79.
32. Chakraborty, M.; Hashmi, M.S.J. An overview of biosensors and devices. *Ref. Mod. Mater. Sci. Mater. Eng.* **2017**, doi:10.1016/b978-0-12-803581-8.10316-9.
33. Dong, J.; Zhao, H.; Xu, M.; Maa, Q.; Ai, S. A label-free electrochemical impedance immunosensor based on AuNPs/PAMAM-MWCNT-Chi nanocomposite modified glassy carbon electrode for detection of *Salmonella typhimurium* in milk. *Food Chem.* **2013**, *141*, 1980–1986.
34. Lin, Y.H.; Chen, S.H.; Chuang, Y.C.; Lu, Y.C.; Shen, T.Y.; Chang, C.A.; Lin, C.S. Disposable amperometric immunosensing strips fabricated by Au nanoparticles-modified screen-printed carbon electrodes for the detection of foodborne pathogen *Escherichia coli* O157:H7. *Biosens. Bioelectron.* **2008**, *23*, 1832–1837.
35. Mathelié-Guinlet, M.; Cohen-Bouhacina, T.; Gammoudi, I.; Martin, A.; Béven, L.; Delville, M.H.; Grauby-Heywang, C. Silica nanoparticles-assisted electrochemical biosensor for the rapid, sensitive and specific detection of *Escherichia coli*. *Sens. Actuator B* **2019**, *292*, 314–320.
36. Chen, S.H.; Wu, V.C.H.; Chuang, Y.C.; Lin, C.S. Using oligonucleotide-functionalized Au nanoparticles to rapidly detect foodborne pathogens on a piezoelectric biosensor. *J. Microbiol. Method* **2008**, *73*, 7–17.
37. Kalograiaki, I.; Euba, B.; Proverbio, D.; Campanero-Rhodes, M.A.; Aastrup, T.; Garmendia, J.; Solís, D. Combined bacteria microarray and quartz crystal microbalance approach for exploring glycosignatures of nontypeable *Haemophilus influenzae* and recognition by host lectins. *Anal. Chem.* **2016**, *88*, 5950–5957.
38. Ma, F.; Rehman, A.; Liu, H.; Zhang, J.; Zhu, S.; Zeng, X. Glycosylation of quinone-fused polythiophene for reagentless and label-free detection of *E. coli*. *Anal. Chem.* **2015**, *87*, 1560–1568.

39. Yoo, S.M.; Lee, S.Y. Optical biosensors for the detection of pathogenic microorganisms. *Trend Biotechnol.* **2016**, *34*, 7–25.
40. Dudak, F.C.; Boyaci, I.H. Rapid and label-free bacteria detection by surface plasmon resonance (SPR) biosensors. *Biotechnol. J.* **2009**, *4*, 1003–1011.
41. Bhunia, A.K. Biosensors and bio-based methods for the separation and detection of foodborne pathogens. *Adv. Food Nutr. Res.* **2008**, *54*, 1–44.
42. Chen, C.; Wang, J. Optical biosensors: An exhaustive and comprehensive review. *Analyst* **2020**, *145*, 1605–1628.
43. Angelopoulou, M.; Kakabakos, S.; Petrou, P. Label-free biosensors based onto monolithically integrated onto silicon optical transducers. *Chemosensors* **2018**, *6*, 52.
44. Sanvicens, N.; Pastells, C.; Pascual, N.; Marco, M.P. Nanoparticle-based biosensors for detection of pathogenic bacteria. *TrAC - Trend Anal. Chem.* **2009**, *28*, 1243–1252.
45. Wang, X.D.; Wolfbeis, O.S. Fiber-optic chemical sensors and biosensors (2008-2012). *Anal. Chem.* **2013**, *85*, 487–508.
46. Benito-Peña, E.; Valdés, M.G.; Glahn-Martínez, B.; Moreno-Bondi, M.C. Fluorescence based fiber optic and planar waveguide biosensors. A review. *Anal. Chim. Acta* **2016**, *943*, 17-40.
47. Taitt, C.R.; Anderson, G.P.; Ligler, F.S. Evanescent wave fluorescence biosensors: Advances of the last decade. *Biosens. Bioelectron.* **2016**, *76*, 103-112.
48. Vashist, S.K.; Lippa, P.B.; Yeo, L.Y.; Ozcan, A.; Luong, J.H.T. Emerging technologies for next-generation Point-of-Care testing. *Trend Biotechnol.* **2015**, *33*, 692–705.
49. Gauglitz, G. Direct optical detection in bioanalysis: An update. *Anal. Bioanal. Chem.* **2010**, *398*, 2363–2372.
50. Luan, E.; Shoman, H.; Ratner, D.M.; Cheung, K.C.; Chrostowski, L. Silicon photonic biosensors using label-free detection. *Sensors* **2018**, *18*, 3519.
51. Lee, D.; Hwang, J.; Seo, Y.; Gilad, A.A.; Choi, J. Optical immunosensors for the efficient detection of target biomolecules. *Biotechnol. Bioproc. Eng.* **2018**, *23*, 123–133.
52. Huertas, C.S.; Calvo-Lozano, O.; Mitchell, A.; Lechuga, L.M. Advanced evanescent-wave optical biosensors for the detection of nucleic acids: An analytic perspective. *Front. Chem.* **2019**, *7*, 724.
53. Gauglitz, G.; Nahm, W. Observation of spectral interferences for the determination of volume and surface effects of thin films. *Fresenius J. Anal. Chem.* **1991**, *341*, 279–283.
54. Rothmund, M.; Schütz, A.; Brecht, A.; Gauglitz, G.; Berthel, G.; Gräfe, D. Label free binding assay with spectroscopic detection for pharmaceutical screening. *Fresenius J. Anal. Chem.* **1997**, *359*, 15–22.
55. Bleher, O.; Schindler, A.; Yin, M.X.; Holmes, A.B.; Lippa, P.B.; Gauglitz, G.; Proll, G. Development of a new parallelized, optical biosensor platform for label-free detection of autoimmunity-related antibodies multiplex platforms in diagnostics and bioanalytics. *Anal. Bioanal. Chem.* **2014**, *406*, 3305–3314.
56. Schwartz, M.P.; Alvarez, S.D.; Sailor, M.J. A Porous SiO<sub>2</sub> interferometric biosensor for quantitative determination of protein interactions: Binding of protein A to immunoglobulins derived from different species. *Anal. Chem.* **2007**, *79*, 327-334.
57. Tsang, C.K.; Kelly, T.L.; Sailor, M.J.; Li, Y.Y. Highly stable porous silicon-carbon composites as label-free optical biosensors. *ACS Nano* **2012**, *6*, 10546–10554.
58. Mun, K.S.; Alvarez, S.D.; Choi, W.Y.; Sailor, M.J. A Stable, label-free optical interferometric biosensor based on TiO<sub>2</sub> nanotube arrays. *ACS Nano* **2010**, *4*, 2070–2076.
59. Petrou, P.S.; Ricklin, D.; Zavali, M.; Raptis, I.; Kakabakos, S.E.; Misiakos, K.; Lambris, J.D. Real-time label-free detection of complement activation products in human serum by White Light Reflectance Spectroscopy. *Biosens. Bioelectron.* **2009**, *24*, 3359–3364.
60. Tsounidi, D.; Koukouvinos, G.; Petrou, P.; Misiakos, K.; Zisis, G.; Goustouridis, D.; Raptis, I.; Kakabakos, S.E. Rapid and sensitive label-free determination of aflatoxin M1 levels in milk through a White Light Reflectance Spectroscopy immunosensor. *Sens. Actuator B* **2019**, *282*, 104–111.
61. Koukouvinos, G.; Petrou, P.; Goustouridis, D.; Misiakos, K.; Kakabakos, S.; Raptis, I. Development and bioanalytical applications of a White Light Reflectance Spectroscopy label-free sensing platform. *Biosensors* **2017**, *7*, 46
62. Kurihara, Y.; Takama, M.; Masubuchi, M.; Ooya, T.; Takeuchi, T. Microfluidic reflectometric interference spectroscopy-based sensing for exploration of protein-protein interaction conditions. *Biosens. Bioelectron.* **2013**, *40*, 247–251.
63. Fratamico, P.M.; Strobaugh, T.R.; Medina, M.B.; Gehring, A.G. Detection of *Escherichia coli* 0157:H7 using a surface plasmon resonance biosensor. *Biotechnol. Technique* **1998**, *12*, 571–576.
64. Jyoung, J.-Y.; Hong, S.H.; Lee, W.; Choi, J.W. Immunosensor for the detection of *Vibrio cholerae* O1 using surface plasmon resonance. *Biosens. Bioelectron.* **2006**, *21*, 2315–2319.

65. Oh, B.K.; Kim, Y.K.; Lee, W.; Bae, Y.M.; Lee, W.H.; Choi, J.W. Immunosensor for detection of *Legionella pneumophila* using surface plasmon resonance. *Biosens. Bioelectron.* **2003**, *18*, 605–611.
66. Waswa, J.W.; Debroy, C.; Irudayaraj, J. Rapid detection of *Salmonella* Enteritidis and *Escherichia Coli* using surface plasmon resonance biosensor. *J. Food Proc. Eng.* **2006**, *29*, 373–385.
67. Bokken, G.C.A.M.; Corbee, R.J.; Van Knapen, F.; Bergwerff, A.A. Immunochemical detection of *Salmonella* group B, D and E using an optical surface plasmon resonance biosensor. *FEMS Microbiol. Lett.* **2003**, *222*, 75–82.
68. Subramanian, A.; Irudayaraj, J.; Ryan, T. Mono and dithiol surfaces on surface plasmon resonance biosensors for detection of *Staphylococcus aureus*. *Sens. Actuator B* **2006**, *114*, 192–198.
69. Subramanian, A.; Irudayaraj, J.; Ryan, T. A Mixed self-assembled monolayer-based surface plasmon immunosensor for detection of *E. coli* O157:H7. *Biosens. Bioelectron.* **2006**, *21*, 998–1006.
70. Oh, B.K.; Lee, W.; Kim, Y.K.; Lee, W.H.; Choi, J.W. Surface plasmon resonance immunosensor using self-assembled protein G for the detection of *Salmonella paratyphi*. *J. Biotechnol.* **2004**, *111*, 1–8.
71. Vaisocherová-Lísalová, H.; Víšová, I.; Ermini, M.L.; Špringer, T.; Song, X.C.; Mrázek, J.; Lamačová, J.; Scott Lynn, N.; Šedivák, P.; Homola, J. Low-fouling surface plasmon resonance biosensor for multi-step detection of foodborne bacterial pathogens in complex food samples. *Biosens. Bioelectron.* **2016**, *80*, 84–90.
72. Masdor, N.A.; Altintas, Z.; Tothill, I.E. Surface plasmon resonance immunosensor for the detection of *Campylobacter jejuni*. *Chemosensors* **2017**, *5*, 16.
73. Poltronieri, P.; De Blasi, M.D.; D’Urso, O.F. Detection of *Listeria monocytogenes* through real-time PCR and biosensor methods. *Plant Soil Environ.* **2009**, *55*, 363–369.
74. Linman, M.J.; Sugerman, K.; Cheng, Q. Detection of low levels of *Escherichia coli* in fresh spinach by surface plasmon resonance spectroscopy with a TMB-based enzymatic signal enhancement method. *Sens. Actuator B* **2010**, *145*, 613–619.
75. Makhneva, E.; Farka, Z.; Skládal, P.; Zajíčková, L. Cyclopropylamine plasma polymer surfaces for label-free SPR and QCM immunosensing of *Salmonella*. *Sens. Actuator B* **2018**, *276*, 447–455.
76. Taylor, A.D.; Yu, Q.; Chen, S.; Homola, J.; Jiang, S. Comparison of *E. coli* O157:H7 preparation methods used for detection with surface plasmon resonance sensor. *Sens. Actuator B* **2005**, *107*, 202–208.
77. Waswa, J.; Irudayaraj, J.; DebRoy, C. Direct detection of *E. coli* O157:H7 in selected food systems by a surface plasmon resonance biosensor. *LWT - Food Sci. Technol.* **2007**, *40*, 187–192.
78. Mazumdar, S.D.; Hartmann, M.; Kämpfer, P.; Keusgen, M. Rapid method for detection of *Salmonella* in milk by surface plasmon resonance (SPR). *Biosens. Bioelectron.* **2007**, *22*, 2040–2046.
79. Leonard, P.; Hearty, S.; Quinn, J.; O’Kennedy, R. A generic approach for the detection of whole *Listeria monocytogenes* cells in contaminated samples using surface plasmon resonance. *Biosens. Bioelectron.* **2004**, *19*, 1331–1335.
80. Wang, Y.; Ye, Z.; Si, C.; Ying, Y. Subtractive inhibition assay for the detection of *E. coli* O157:H7 using surface plasmon resonance. *Sensors* **2011**, *11*, 2728–2739.
81. Wang, D.B.; Bi, L.J.; Zhang, Z.P.; Chen, Y.Y.; Yang, R.F.; Wei, H.P.; Zhou, Y.F.; Zhang, X.E. Label-free detection of *B. anthracis* spores using a surface plasmon resonance biosensor. *Analyst* **2009**, *134*, 738–742.
82. Skottrup, P.D.; Nicolaisen, M.; Justesen, A.F. Towards on-site pathogen detection using antibody-based sensors. *Biosens. Bioelectron.* **2008**, *24*, 339–348.
83. Skottrup, P.; Nicolaisen, M.; Justesen, A.F. Rapid determination of *Phytophthora infestans* sporangia using a surface plasmon resonance immunosensor. *J. Microbiol. Method* **2007**, *68*, 507–515.
84. Skottrup, P.; Hearty, S.; Frøkiær, H.; Leonard, P.; Hejgaard, J.; O’Kennedy, R.; Nicolaisen, M.; Justesen, A.F. Detection of fungal spores using a generic surface plasmon resonance immunoassay. *Biosens. Bioelectron.* **2007**, *22*, 2724–2729.
85. Kang, C.D.; Cao, C.; Lee, J.; Choi, I.S.; Kim, B.W.; Sim, S.J. Surface plasmon resonance-based inhibition assay for real-time detection of *Cryptosporidium parvum* oocyst. *Water Res.* **2008**, *42*, 1693–1699.
86. Leonard, P.; Hearty, S.; Wyatt, G.; Quinn, J.; O’Kennedy, R. Development of a surface plasmon resonance-based immunoassay for *Listeria monocytogenes*. *J. Food Protect.* **2005**, *68*, 728–735.
87. Oh, B.K.; Lee, W.; Chun, B.S.; Bae, Y.M.; Lee, W.H.; Choi, J.W. The fabrication of protein chip based on surface plasmon resonance for detection of pathogens. *Biosens. Bioelectron.* **2005**, *20*, 1847–1850.
88. Taylor, A.D.; Ladd, J.; Yu, Q.; Chen, S.; Homola, J.; Jiang, S. Quantitative and simultaneous detection of four foodborne bacterial pathogens with a multi-channel SPR sensor. *Biosens. Bioelectron.* **2006**, *22*, 752–758.
89. Morlay, A.; Duquenoy, A.; Piat, F.; Calemczuk, R.; Mercey, T.; Livache, T.; Roupioz, Y. Label-free immunosensors for the fast detection of *Listeria* in Food. *Measurement* **2017**, *98*, 305–310.
90. Chen, J.; Park, B. Label-free screening of foodborne *Salmonella* using surface plasmon resonance imaging. *Anal. Bioanal. Chem.* **2018**, *410*, 5455–5464.

91. Park, B.; Wang, B.; Chen, J. Label-free immunoassay for multiplex detections of foodborne bacteria in chicken carcass rinse with surface plasmon resonance imaging. *Foodborne Pathog. Dis.* **2021**, *18*, 202-209.
92. Boulade, M.; Morlay, A.; Piat, F.; Roupioz, Y.; Livache, T.; Charette, P.G.; Canva, M.; Leroy, L. Early detection of bacteria using SPR imaging and event counting: Experiments with *Listeria monocytogenes* and *Listeria innocua*. *RSC Advances* **2019**, *9*, 15554–15560.
93. Wei, D.; Oyarzabal, O.A.; Huang, T.S.; Balasubramanian, S.; Sista, S.; Simonian, A.L. Development of a surface plasmon resonance biosensor for the identification of *Campylobacter jejuni*. *J. Microbiol. Method* **2007**, *69*, 78–85.
94. Meeusen, C.A.; Alocilja, E.C.; Osburn, W.N. Detection of *E. coli* O157:H7 using a miniaturized surface plasmon resonance biosensor. *Transact. ASAE* **2005**, *48*, 2409–2416.
95. Dudak, F.C.; Boyaci, I.H. Development of an immunosensor based on surface plasmon resonance for enumeration of *Escherichia coli* in water samples. *Food Res. Int.* **2007**, *40*, 803–807.
96. Lan, Y. -B; Wang, S.-Z; Yin, Y.-G.; Hoffmann, W.C.; Zheng, X.-Z. Using a surface plasmon resonance biosensor for rapid detection of *Salmonella typhimurium* in chicken carcass. *J. Bionic Eng.* **2008**, *5*, 239–246.
97. Torun, Ö.; Hakki Boyaci, I.; Temür, E.; Tamer, U. Comparison of sensing strategies in SPR biosensor for rapid and sensitive enumeration of bacteria. *Biosens. Bioelectron.* **2012**, *37*, 53–60.
98. Tokel, O.; Yildiz, U.H.; Inci, F.; Durmus, N.G.; Ekiz, O.O.; Turker, B.; Cetin, C.; Rao, S.; Sridhar, K.; Natarajan, N.; et al. Portable microfluidic integrated plasmonic platform for pathogen detection. *Sci. Rep.* **2015**, *5*, 9154.
99. Nguyen, H.H.; Yi, S.Y.; Woubit, A.; Kim, M. A portable surface plasmon resonance biosensor for rapid detection of *Salmonella typhimurium*. *Appl. Sci. Converg. Technol.* **2016**, *25*, 61–65.
100. Choi, J.; Lee, J.; Son, J.; Choi, J. Noble metal-assisted surface plasmon resonance immunosensors. *Sensors* **2020**, *20*, 1003.
101. Lopez, G.A.; Estevez, M.C.; Soler, M.; Lechuga, L.M. Recent advances in nanoplasmonic biosensors: Applications and lab-on-a-chip integration. *Nanophotonics* **2017**, *6*, 123–136.
102. Fu, J.; Park, B.; Zhao, Y. Limitation of a localized surface plasmon resonance sensor for *Salmonella* detection. *Sens. Actuator B* **2009**, *141*, 276–283.
103. Song, L.; Zhang, L.; Huang, Y.; Chen, L.; Zhang, G.; Shen, Z.; Zhang, J.; Xiao, Z.; Chen, T. Amplifying the signal of localized surface plasmon resonance sensing for the sensitive detection of *Escherichia coli* O157:H7. *Sci. Rep.* **2017**, *7*, 1–8.
104. Yaghubi, F.; Zeinoddini, M.; Saeedinia, A.R.; Azizi, A.; Samimi Nemati, A. Design of localized surface plasmon resonance (LSPR) biosensor for immunodiagnostic of *E. coli* O157:H7 using gold nanoparticles conjugated to the chicken antibody. *Plasmonics* **2020**, *15*, 1481–1487.
105. Wang, Y.; Knoll, W.; Dostalek, J. Bacterial pathogen surface plasmon resonance biosensor advanced by long range surface plasmons and magnetic nanoparticle assays. *Anal. Chem.* **2012**, *84*, 8345–8350.
106. Sharma, H.; Mutharasan, R. Review of biosensors for foodborne pathogens and toxins. *Sens. Actuator B* **2013**, *183*, 535–549.
107. Rijal, K.; Leung, A.; Shankar, P.M.; Mutharasan, R. Detection of pathogen *Escherichia coli* O157:H7 at 70 cells/mL using antibody-immobilized biconical tapered fiber sensors. *Biosens. Bioelectron.* **2005**, *21*, 871–880.
108. Wiejata, P.J.; Shankar, P.M.; Mutharasan, R. Fluorescent sensing using biconical tapers. *Sens. Actuator B* **2003**, *96*, 315–320.
109. Yu, W.; Lang, T.; Bian, J.; Kong, W. Label-free fiber optic biosensor based on thin-core modal interferometer. *Sens. Actuator B* **2016**, *228*, 322–329.
110. Bharadwaj, R.; Sai, V.V.R.; Thakare, K.; Dhawangale, A.; Kundu, T.; Titus, S.; Verma, P.K.; Mukherji, S. Evanescent wave absorbance based fiber optic biosensor for label-free detection of *E. coli* at 280 nm wavelength. *Biosens. Bioelectron.* **2011**, *26*, 3367–3370.
111. Wandemur, G.; Rodrigues, D.; Allil, R.; Queiroz, V.; Peixoto, R.; Werneck, M.; Miguel, M. Plastic optical fiber-based biosensor platform for rapid cell detection. *Biosens. Bioelectron.* **2014**, *54*, 661–666.
112. Zhou, C.; Pivarnik, P.; Auger, S.; Rand, A.; Letcher, S. A compact fiber-optic immunosensor for *Salmonella* based on evanescent wave excitation. *Sens. Actuator B* **1997**, *42*, 169–175.
113. Geng, T.; Uknalis, J.; Tu, S.I.; Bhunia, A.K. Fiber-optic biosensor employing Alexa-Fluor conjugated antibody for detection of *Escherichia coli* O157:H7 from ground beef in four hours. *Sensors* **2006**, *6*, 796–807.
114. Kramer, M.F.; Lim, D.V. A rapid and automated fiber optic-based biosensor assay for the detection of *Salmonella* in spent irrigation water used in the sprouting of sprout seeds. *J. Food Protect.* **2004**, *67*, 46–52.
115. Leskinen, S.D.; Lim, D.V. Rapid ultrafiltration concentration and biosensor detection of *Enterococci* from large volumes of Florida recreational water. *Appl. Environ. Microbiol.* **2008**, *74*, 4792-4798.

116. Geng, T.; Morgan, M.T.; Bhunia, A.K. Detection of low levels of *Listeria monocytogenes* cells by using a fiber-optic immunosensor. *Appl. Environ. Microbiol.* **2004**, *70*, 6138–6146.
117. Ohk, S.H.; Koo, O.K.; Sen, T.; Yamamoto, C.M.; Bhunia, A.K. Antibody-aptamer functionalized fibre-optic biosensor for specific detection of *Listeria monocytogenes* from food. *J. Appl. Microbiol.* **2010**, *109*, 808–817.
118. Nanduri, V.; Kim, G.; Morgan, M.T.; Ess, D.; Hahm, B.K.; Kothapalli, A.; Valadez, A.; Geng, T.; Bhunia, A.K. Antibody immobilization on waveguides using a flow-through system shows improved *Listeria monocytogenes* detection in an automated fiber optic biosensor: RAPTOR™. *Sensors* **2006**, *6*, 808–822.
119. Ohk, S.H.; Bhunia, A.K. Multiplex fiber optic biosensor for detection of *Listeria monocytogenes*, *Escherichia coli* O157: H7 and *Salmonella enterica* from ready-to-eat meat samples. *Food Microbiol.* **2013**, *33*, 166–171.
120. Ko, S.; Grant, S.A. A Novel FRET-based optical fiber biosensor for rapid detection of *Salmonella typhimurium*. *Biosens. Bioelectron.* **2006**, *21*, 1283–1290.
121. Fallah, H.; Asadishad, T.; Parsanasab, G.M.; Harun, S.W.; Mohammed, W.S.; Yasin, M. Optical fiber biosensor toward E-coli bacterial detection on the pollutant water. *Eng. J.* **2021**, *25*, 1–8.
122. Lin, H.Y.; Tsao, Y.C.; Tsai, W.H.; Yang, Y.W.; Yan, T.R.; Sheu, B.C. Development and application of side-polished fiber immunosensor based on surface plasmon resonance for the detection of *Legionella pneumophila* with halogens light and 850 nm-LED. *Sens. Actuators A* **2007**, *138*, 299–305.
123. Kaushik, S.; Tiwari, U.K.; Pal, S.S.; Sinha, R.K. Rapid detection of *Escherichia coli* using fiber optic surface plasmon resonance immunosensor based on biofunctionalized molybdenum disulfide (MoS<sub>2</sub>) nanosheets. *Biosens. Bioelectron.* **2019**, *126*, 501–509.
124. Kozma, P.; Kehl, F.; Ehrentreich-Förster, E.; Stamm, C.; Bier, F.F. Integrated planar optical waveguide interferometer biosensors: A comparative review. *Biosens. Bioelectron.* **2014**, *58*, 287–307.
125. Makarona E., Petrou P., Kakabakos S., Misiakos K., Raptis I. Point-of-need bioanalytics based on planar optical interferometry. *Biotechnol. Adv.* **2016**, *34*, 209–233
126. Sarkar, D.; Gunda, N.S.K.; Jamal, I.; Mitra, S.K. Optical biosensors with an integrated Mach-Zehnder interferometer for detection of *Listeria monocytogenes*. *Biomed. Microdev.* **2014**, *16*, 509–520.
127. Mathesz, A.; Valkai, S.; Újvárosy, A.; Aekbote, B.; Sipos, O.; Stercz, B.; Kocsis, B.; Szabó, D.; Dér, A. Integrated optical biosensor for rapid detection of bacteria. *Optofluid. Microfluid. Nanofluid.* **2016**, *2*, 15–21.
128. Angelopoulou, M.; Petrou, P.; Misiakos, K.; Raptis, I.; Kakabakos, S. Simultaneous detection of *Salmonella typhimurium* and *Escherichia coli* O157:H7 in drinking water and milk with Mach-Zehnder interferometers monolithically integrated on silicon chips. *Biosensors* **2022**, *12*, 507.
129. Ymeti, A.; Greve, J.; Lambeck, P. V.; Wink, T.; Van Novell, S.W.F.M.; Beumer, T.A.M.; Wijn, R.R.; Heideman, R.G.; Subramaniam, V.; Kanger, J.S. Fast, ultrasensitive virus detection using a Young interferometer sensor. *Nano Lett.* **2007**, *7*, 394–397.
130. Schneider, B.H.; Edwards, J.G.; Hartman, N.F. Hartman interferometer: Versatile integrated optic sensor for label-free, real-time quantification of nucleic acids, proteins, and pathogens. *Clin. Chem.* **1997**, *43*, 1757–1763.
131. Seo, K.H.; Brackett, R.E.; Hartman, N.F.; Campbell, D.P. Development of a rapid response biosensor for detection of *Salmonella typhimurium*. *J. Food Protect.* **1999**, *62*, 431–437.
132. Nagel, T.; Ehrentreich-Förster, E.; Singh, M.; Schmitt, K.; Brandenburg, A.; Berka, A.; Bier, F.F. Direct detection of Tuberculosis infection in blood serum using three optical label-free approaches. *Sens. Actuator B* **2008**, *129*, 934–940.
133. Maldonado, J.; González-Guerrero, A.B.; Domínguez, C.; Lechuga, L.M. Label-free bimodal waveguide immunosensor for rapid diagnosis of bacterial infections in cirrhotic patients. *Biosens. Bioelectron.* **2016**, *85*, 310–316.
134. Maldonado, J.; González-Guerrero, A.B.; Fernández-Gavela, A.; González-López, J.J.; Lechuga, L.M. Ultrasensitive label-free detection of unamplified multidrug-resistance bacteria genes with a bimodal waveguide interferometric biosensor. *Diagnostics* **2020**, *10*, 845.
135. Grego, S.; McDaniel, J.R.; Stoner, B.R. Wavelength interrogation of grating-based optical biosensors in the input coupler configuration. *Sens. Actuator B* **2008**, *131*, 347–355.
136. Adrian, J.; Pasche, S.; Diserens, J.M.; Sánchez-Baeza, F.; Gao, H.; Marco, M.P.; Voirin, G. Waveguide interrogated optical immunosensor (WIOS) for detection of sulfonamide antibiotics in milk. *Biosens. Bioelectron.* **2009**, *24*, 3340–3346.
137. Kehl, F.; Etlinger, G.; Gartmann, T.E.; Tschärner, N.S.R.U.; Heub, S.; Follonier, S. Introduction of an angle interrogated, MEMS-based, optical waveguide grating system for label-free biosensing. *Sens. Actuator B* **2016**, *226*, 135–143.

138. Kozma, P.; Hamori, A.; Cottier, K.; Kurunczi, S.; Horvath, R. Grating coupled interferometry for optical sensing. *Appl. Phys. B* **2009**, *97*, 5–8.
139. Teotia, P.K.; Kaler, R.S. Multilayer with Periodic Grating Based High Performance SPR Waveguide Sensor. *Opt. Commun.* **2017**, *395*, 154–158.
140. Marusov, G.; Sweatt, A.; Pietrosimone, K.; Benson, D.; Geary, S.J.; Silbart, L.K.; Challa, S.; Lagoy, J.; Lawrence, D.A.; Lynes, M.A. A microarray biosensor for multiplexed detection of microbes using grating-coupled surface plasmon resonance imaging. *Environ. Sci. Technol.* **2012**, *46*, 348–359.
141. Davies, E.; Viitala, R.; Salomäki, M.; James, S.W.; Tatam, R.P. Optical fibre long-period grating sensors: Characteristics and application. *Meas. Sci. Technol.* **2003**, *14*, R49.
142. Shi, W.; Wang, X.; Zhang, W.; Yun, H.; Lin, C.; Chrostowski, L.; Jaeger, N.A.F. Grating-coupled silicon microring resonators. *Appl. Phys. Lett.* **2012**, *100*, 121118.
143. Horváth, R.; Pedersen, H.C.; Skivesen, N.; Selmeczi, D.; Larsen, N.B. Optical waveguide sensor for on-line monitoring of bacteria. *Opt. Lett.* **2003**, *28*, 1233.
144. Bandara, A.B.; Zuo, Z.; Ramachandran, S.; Ritter, A.; Heflin, J.R.; Inzana, T.J. Detection of methicillin-resistant Staphylococci by biosensor assay consisting of nanoscale films on optical fiber long-period gratings. *Biosens. Bioelectron.* **2015**, *70*, 433–440.
145. Yang, F.; Chang, T.L.; Liu, T.; Wu, D.; Du, H.; Liang, J.; Tian, F. Label-free detection of Staphylococcus aureus bacteria using long-period fiber gratings with functional polyelectrolyte coatings. *Biosens. Bioelectron.* **2019**, *133*, 147–153.
146. Kaushik, S.; Tiwari, U.; Nilima; Prashar, S.; Das, B.; Sinha, R.K. Label-free detection of Escherichia coli bacteria by cascaded chirped long period gratings immunosensor. *Rev. Sci. Instr.* **2019**, *90*, 025003.
147. Kim, N.; Park, I.S.; Kim, W.Y. Salmonella detection with a direct-binding optical grating coupler immunosensor. *Sens. Actuator B* **2007**, *121*, 606–615.
148. Cooper, I.R.; Meikle, S.T.; Standen, G.; Hanlon, G.W.; Santin, M. The rapid and specific real-time detection of Legionella pneumophila in water samples using optical waveguide lightmode spectroscopy. *J. Microbiol. Method* **2009**, *78*, 40–44.
149. Lee, S.; Chan Eom, S.; Soo Chang, J.; Huh, C.; Yong Sung, G.; Shin, J.H. A silicon nitride microdisk resonator with a 40-nm-thin horizontal air slot. *Opt. Exp.* **2010**, *18*, 11209–11215.
150. De Vos, K.; Bartolozzi, I.; Schacht, E.; Bienstman, P.; Baets, R. Silicon-on-insulator microring resonator for sensitive and label-free biosensing. *Opt. Exp.* **2007**, *15*, 7610–7615.
151. Armani, D.K.; Kippenberg, T.J.; Spillane, S.M.; Vahala, K.J. Ultra-high-Q toroid microcavity on a chip. *Nature* **2003**, *421*, 925–928.
152. Ramachandran, A.; Wang, S.; Clarke, J.; Ja, S.J.; Goad, D.; Wald, L.; Flood, E.M.; Knobbe, E.; Hryniewicz, J. V.; Chu, S.T.; Gill, D.; Chen, W.; King, O.; Little, B.E. A universal biosensing platform based on optical micro-ring resonators. *Biosens. Bioelectron.* **2008**, *23*, 939–944.
153. Ghali, H.; Chibli, H.; Nadeau, J.L.; Bianucci, P.; Peter, Y.A. Real-time detection of Staphylococcus aureus using whispering gallery mode optical microdisks. *Biosensors* **2016**, *6*, 20.
154. Merkl, S.; Vornicescu, D.; Dassinger, N.; Keusgen, M. Detection of whole cells using reflectometric interference spectroscopy. *Phys. Status Solidi A* **2014**, *211*, 1416–1422.
155. Angelopoulou, M.; Tziaila, K.; Voulgari, A.; Dikeoulia, M.; Raptis, I.; Kakabakos, S.E.; Petrou, P. Rapid detection of Salmonella typhimurium in drinking water by a White Light Reflectance Spectroscopy immunosensor. *Sensors* **2021**, *21*, 2683.
156. Massad-Ivanir, N.; Shtenberg, G.; Tzur, A.; Krepker, M.A.; Segal, E. Engineering nanostructured porous SiO<sub>2</sub> surfaces for bacteria detection via “direct cell capture.” *Anal. Chem.* **2011**, *83*, 3282–3289.
157. Massad-Ivanir, N.; Shtenberg, G.; Segal, E. Optical detection of E. coli Bacteria by Mesoporous Silicon Biosensors. *J. Vis. Exp.* **2013**, 6–13.
158. Massad-Ivanir, N.; Shtenberg, G.; Raz, N.; Gazenbeek, C.; Budding, D.; Bos, M.P.; Segal, E. Porous silicon-based biosensors: Towards real-time optical detection of target bacteria in the food industry. *Sci. Rep.* **2016**, *6*, 38099.
159. Massad-Ivanir, N.; Shtenberg, G.; Segal, E. Advancing nanostructured porous Si-based optical transducers for label free bacteria detection. *Adv. Exp. Med. Biol.* **2012**, *733*, 37–45.
160. Tang, Y.; Li, Z.; Luo, Q.; Liu, J.; Wu, J. Bacteria detection based on its blockage effect on silicon nanopore array. *Biosens. Bioelectron.* **2016**, *79*, 715–720.
161. Zaraee, N.; Kanik, F.E.; Bhuiya, A.M.; Gong, E.S.; Geib, M.T.; Lortlar Ünlü, N.; Ozkumur, A.Y.; Dupuis, J.R.; Ünlü, M.S. Highly sensitive and label-free digital detection of whole cell E. coli with interferometric reflectance imaging. *Biosens. Bioelectron.* **2020**, *162*, 112258.

162. Reardon, K.F.; Zhong, Z.; Lear, K.L. Environmental applications of photoluminescence-based biosensors. In *Optical Sensor Systems in Biotechnology*, Rao, G., Volume Editor; Springer-Verlag Berlin Heidelberg, Germany, 2009; Volume 116, pp. 99–123.
163. Viter, R.; Tereshchenko, A.; Smyntyna, V.; Ogorodniichuk, J.; Starodub, N.; Yakimova, R.; Khranovskyy, V.; Ramanavicius, A. Toward development of optical biosensors based on photoluminescence of TiO<sub>2</sub> nanoparticles for the detection of Salmonella. *Sens. Actuator B* **2017**, *252*, 95–102.
164. Taitt, C.R.; Shubin, Y.S.; Angel, R.; Ligler, F.S. Detection of Salmonella enterica serovar typhimurium by using a rapid, array-based immunosensor. *Appl. Environ. Microbiol.* **2004**, *70*, 152–158.
165. Sapsford, K.E.; Rasooly, A.; Taitt, C.R.; Ligler, F.S. Detection of Campylobacter and Shigella Species in Food Samples Using an Array Biosensor. *Analytical Chemistry* **2004**, *76*, 433–440.
166. Sapsford, K.E.; Ngundi, M.M.; Moore, M.H.; Lassman, M.E.; Shriver-Lake, L.C.; Taitt, C.R.; Ligler, F.S. Rapid detection of foodborne contaminants using an array biosensor. *Sens. Actuators B* **2006**, *113*, 599–607.
167. Shriver-Lake, L.C.; Turner, S.; Taitt, C.R. Rapid detection of Escherichia coli O157:H7 spiked into food matrices. *Anal. Chim. Acta* **2007**, *584*, 66–71.
168. Dehghani, Z.; Mohammadnejad, J.; Hosseini, M.; Bakhshi, B.; Rezayan, A.H. Whole cell FRET immunosensor based on graphene oxide and graphene dot for Campylobacter jejuni detection. *Food Chem.* **2020**, *309*, 125690.
169. Wang, Z.; Zong, S.; Wu, L.; Zhu, D.; Cui, Y. SERS-activated platforms for immunoassay: Probes, encoding methods, and applications. *Chem. Rev.* **2017**, *117*, 7910–7963.
170. Mosier-Boss, P.A. Review on SERS of bacteria. *Biosensors* **2017**, *7*, 51.
171. Zhou, X.; Hu, Z.; Yang, D.; Xie, S.; Jiang, Z.; Niessner, R.; Haisch, C.; Zhou, H.; Sun, P. Bacteria detection: From powerful SERS to its advanced compatible techniques. *Adv. Science* **2020**, *7*, 2001739.
172. Qu, L.L.; Ying, Y.L.; Yu, R.J.; Long, Y.T. In situ food-borne pathogen sensors in a nanoconfined space by surface enhanced Raman scattering. *Microchim. Acta* **2021**, *188*, 201.
173. Xie, X.; Pu, H.; Sun, D.W. Recent advances in nanofabrication techniques for SERS substrates and their applications in food safety analysis. *Crit. Rev. Food Sci. Nutr.* **2018**, *58*, 2800–2813.
174. Knauer, M.; Ivleva, N.P.; Liu, X.; Niessner, R.; Haisch, C. Surface-enhanced Raman scattering-based label-free microarray readout for the detection of microorganisms. *Anal. Chem.* **2010**, *82*, 2766–2772.
175. Knauer, M.; Ivleva, N.P.; Niessner, R.; Haisch, C. A flow-through microarray cell for the online SERS detection of antibody-captured E. coli bacteria. *Anal. Bioanal. Chem.* **2012**, *402*, 2663–2667.
176. Cho, I.H.; Bhandari, P.; Patel, P.; Irudayaraj, J. Membrane filter-assisted surface enhanced Raman spectroscopy for the rapid detection of E. coli O157:H7 in ground beef. *Biosens. Bioelectron.* **2015**, *64*, 171–176.
177. Bai, X.; Shen, A.; Hu, J. A sensitive SERS-based sandwich immunoassay platform for simultaneous multiple detection of foodborne pathogens without interference. *Anal. Method* **2020**, *12*, 4885–4891.
178. Najafi, R.; Mukherjee, S.; Hudson, J.; Sharma, A.; Banerjee, P. Development of a rapid capture-cum-detection method for Escherichia coli O157 from apple juice comprising nano-immunomagnetic separation in tandem with surface enhanced Raman scattering. *Int. J. Food Microbiol.* **2014**, *189*, 89–97.
179. Kearns, H.; Goodacre, R.; Jamieson, L.E.; Graham, D.; Faulds, K. SERS detection of multiple antimicrobial-resistant pathogens using nanosensors. *Anal. Chem.* **2017**, *89*, 12666–12673.
180. Wang, J.; Wu, X.; Wang, C.; Rong, Z.; Ding, H.; Li, H.; Li, S.; Shao, N.; Dong, P.; Xiao, R.; Wang, S.-Q. Facile synthesis of Au-coated magnetic nanoparticles and their application in bacteria detection via a SERS method. *ACS Appl. Mater. Interface* **2016**, *8*, 19958–19967.
181. Tamer, U.; Boyaci, I.H.; Temur, E.; Zengin, A.; Dincer, I.; Elerman, Y. Fabrication of magnetic gold nanorod particles for immunomagnetic separation and SERS application. *J. Nanopart. Res.* **2011**, *13*, 3167–3176.
182. Temur, E.; Boyaci, I.H.; Tamer, U.; Unsal, H.; Aydogan, N. A Highly Sensitive detection platform based on surface-enhanced Raman scattering for Escherichia coli enumeration. *Anal. Bioanal. Chem.* **2010**, *397*, 1595–1604.
183. Guven, B.; Basaran-Akgul, N.; Temur, E.; Tamer, U.; Boyaci, I.H. SERS-based sandwich immunoassay using antibody coated magnetic nanoparticles for Escherichia coli enumeration. *Analyst* **2011**, *136*, 740–748.
184. Lin, H.Y.; Huang, C.H.; Hsieh, W.H.; Liu, L.H.; Lin, Y.C.; Chu, C.C.; Wang, S.T.; Kuo, I.T.; Chau, L.K.; Yang, C.Y. On-line SERS detection of single bacterium using novel SERS nanoprobe and a microfluidic dielectrophoresis device. *Small* **2014**, *10*, 4700–4710.
185. Wu, Z. Simultaneous detection of Listeria monocytogenes and Salmonella typhimurium by a SERS-based lateral flow immunochromatographic assay. *Food Anal. Method* **2019**, *12*, 1086–1091.
186. Liu, H.-B.; Du, X.-J.; Zang, Y.-X.; Li, P.; Wang, S. SERS-based lateral flow strip biosensor for simultaneous detection of Listeria monocytogenes and Salmonella enterica serotype enteritidis. *J. Agr. Food Chem.* **2017**, *65*, 10290–10299.

187. Liu, H.-B.; Chen, C.-Y.; Zhang, C.-N.; Du, X.-J.; Li, P.; Wang, S. Functionalized AuMBA@Ag nanoparticles as an optical and SERS dual probe in a lateral flow strip for the quantitative detection of Escherichia coli O157:H7. *J. Food Sci.* **2019**, *84*, 2916–2924.

**Disclaimer/Publisher's Note:** The statements, opinions and data contained in all publications are solely those of the individual author(s) and contributor(s) and not of MDPI and/or the editor(s). MDPI and/or the editor(s) disclaim responsibility for any injury to people or property resulting from any ideas, methods, instructions or products referred to in the content.